Journal of
Medicinal Chemistry

Article

Serendipitous Discovery of Leucine and Methionine Depletion Agents During the Search for Polyamine Transport Inhibitors

Chelsea Lynn Massaro, Jenna Thomas, Houssine Ikhlef,
Sharifa Dinara, Sara Cronk, Holly Moots, and Otto Phanstiel

J. Med. Chem., **Just Accepted Manuscript** • DOI: 10.1021/acs.jmedchem.9b00568 • Publication Date (Web): 18 Feb 2020

Just Accepted

is published by the American Chemical Society. 1155 Sixteenth Street N.W., Washington, DC 20036

Serendipitous Discovery of Leucine and Methionine Depletion Agents During the Search for Polyamine Transport Inhibitors

Chelsea Massaro, Jenna Thomas, Houssine Ikhlef, Sharifa Dinara, Sara Cronk, Holly Moots, and Otto Phanstiel IV*

*Contacting author

Contact Information:

College of Medicine, University of Central Florida

12722 Research Parkway

Orlando, FL 32827

otto.phanstiel@ucf.edu

407-823-6545

Abstract

Targeting polyamine metabolism is a proven anticancer strategy. Cancers often escape the polyamine biosynthesis inhibitors by increased polyamine import. Therefore, there is much interest in identifying polyamine transport inhibitors (PTIs) to be used in combination therapies. In a search for new PTIs, we serendipitously discovered a LAT-1 efflux agonist, which induces intracellular depletion of methionine, leucine, spermidine, and spermine, but not putrescine. Since *S*-adenosylmethioninamine is made from methionine, a loss of intracellular methionine leads to an inability to biosynthesize spermidine and spermine. Importantly, we found that this methionine-depletion approach to polyamine depletion could not be rescued by exogenous polyamines, thereby obviating the need for a PTI. Using ^{3}H-leucine (the gold standard for LAT-1 transport studies) and JPH-203 (a specific LAT-1 inhibitor), we showed that the efflux agonist did not inhibit the uptake of extracellular leucine, but instead facilitated the efflux of intracellular leucine pools.

Introduction

The native polyamines putrescine (Put), spermidine (Spd), and spermine (Spm) are essential growth factors in eukaryotic cells.[1] At physiological pH, these polyamines are nearly fully protonated, allowing them to interact with biological polyanions in the cell including nucleic acids, proteins, and phospholipids. Polyamines are involved in many biological processes including cell replication, translation, transcription, and regulation of specific gene expression.[1-2] In addition, they have roles in the regulation of cell proliferation, apoptosis, and tumorigenesis. An association between high levels of polyamines and rapid proliferation of eukaryotic cells and cancer was reported in 1968 by Russell and Snyder.[3] Tumor cells in particular accumulate high polyamine concentrations, particularly spermidine, and typically exhibit a high ratio of spermidine to spermine.[3-4] Depletion of intracellular spermidine and spermine has been shown to cause growth arrest through the inhibition of translation.[5] Moreover, depletion of these intracellular polyamine pools affects a number of growth-regulating genes, which also contribute to the growth arrest. Thus, maintenance of polyamine homeostasis is critical for cell viability and proliferation.[6] Not surprisingly, many cancers are addicted to polyamines and targeting polyamine metabolism is a validated anti-cancer strategy.[1]

Polyamine homeostasis is maintained through a balance of polyamine biosynthesis, degradation, uptake and export from the cell (Figure 1).[7] The first step in polyamine biosynthesis is the formation of putrescine from ornithine by ornithine decarboxylase (ODC). The amino acid L-ornithine itself can be generated from L-arginine (via arginase) or be imported from the plasma. Due to its short half-life (10-30 minutes in mammalian systems), ODC is regulated at multiple steps from transcription to post-translational modification.[1] ODC activity is often upregulated in human cancers relative to surrounding normal tissues[8] in an effort to increase intratumoral

polyamine pools through the biosynthetic pathway. As such, ODC is a well-established cancer target and α-difluoromethylornithine (DFMO) was developed as an irreversible inhibitor of ODC that suppresses cancer development in animal models.[7] Treatment with DFMO typically results in rapid depletion of intracellular putrescine and spermidine, and growth arrest.[5] Unfortunately, cancers often circumvent DFMO by upregulating polyamine import to replenish their depleted polyamine pools. Polyamine transport inhibitors (PTIs) have been developed to address this DFMO escape pathway.[7] For example, L3.6pl human pancreatic cancer cells treated with DFMO+PTI (see example PTI structure in Figure 2) in the presence of exogenous spermidine (Spd, 1 μM) remained polyamine depleted and had decreased viability, whereas those treated with DFMO+Spd were >90% viable and had increased intracellular polyamine pools.[7]

Spermidine and spermine biosynthesis requires the addition of an aminopropyl group onto a putrescine or spermidine substrate, respectively.[1] This aminopropyl group is derived from L-methionine. Specifically, L-methionine is converted to *S*-adenosyl-L-methionine (SAM) via methionine adenosyltransferase (MAT). SAM is then decarboxylated by *S*-adenosylmethionine decarboxylase (AdoMetDC) to form *S*-adenosylmethioninamine, i.e., decarboxylated AdoMet.[9] Two aminopropyltransferases, spermidine synthase (SRM) and spermine synthase (SMS), transfer an aminopropyl moiety from *S*-adenosylmethioninamine to their respective substrates (putrescine or spermidine) to form spermidine and spermine. Therefore, rapidly dividing cells must convert some their intracellular methionine pools towards SAM and *S*-adenosylmethioninamine formation to drive polyamine biosynthesis. In summary, polyamine biosynthesis is directly linked to L-ornithine and L-methionine availability.

Polyamine catabolism involves spermine/spermidine N^1-acetyltransferase (SAT1), which catalyzes the formation of N^1-acetylspermine and N^1-acetylspermidine by transferring the acetyl

moiety from acetyl-coenzyme A (acetyl-CoA) to the N^1 position of spermine or spermidine. Acetylpolyamine oxidase (APAO) then catalyzes the conversion of these acetylated polyamines to spermidine or putrescine, respectively, via oxidative cleavage.[2] Alternatively, spermine oxidase (SMOX) can directly convert spermine to spermidine.[1] In addition to being converted to spermidine or putrescine, the *N*-acetylated polyamine products of SAT1 reactions can also be exported from the cells. In this regard, cells have the ability to maintain polyamine homeostasis though modulation of polyamine biosynthesis, transport, and catabolism (Figure 1).[8]

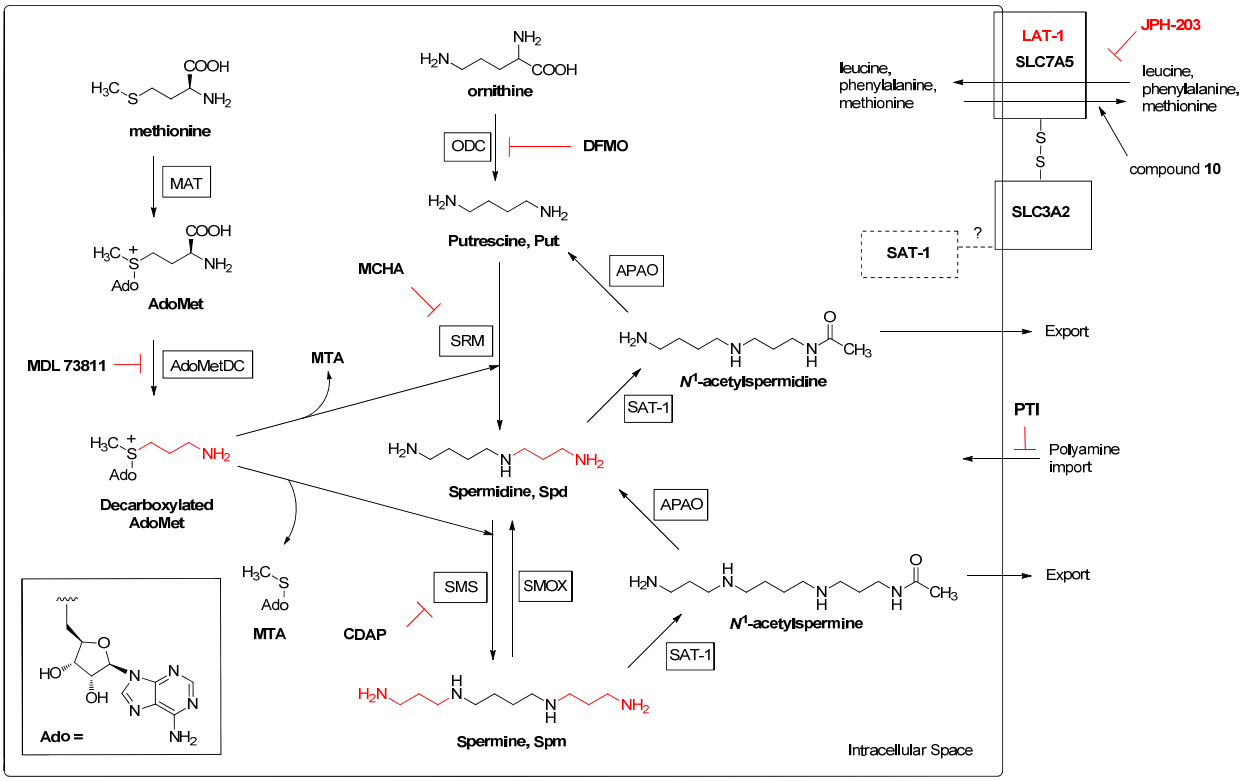

Figure 1. Polyamine Metabolism and import of amino acids by LAT-1.

There has been strong interest in developing inhibitors of polyamine metabolism to control cancer cell growth.[10] In addition to DFMO (**1**), *trans*-4-methylcyclohexylamine (MCHA, **2**) and *N*-(3-aminopropyl)cyclohexylamine (CDAP, **3**) have been developed as competitive inhibitors of

the spermidine and spermine synthases, respectively[11, 12] (see Figure 2). The transition state analogues, S-adenosyl-1,8-diamino-3-thio-octane (AdoDATO) and adenosylspermidine, have also shown promise as spermidine synthase inhibitors.[13] However, cancer cells can modulate/interconvert their polyamine pools or increase polyamine uptake to address these interventions.[12] PTIs like the one shown in Figure 2 (**4**) have been shown to be effective in depleting cells of polyamines when used in combination with DFMO even in the presence of exogenous spermidine.[7] Indeed, this combination of a polyamine biosynthesis inhibitor and a PTI has been shown to significantly increase survival in an orthotopic mouse model of pancreatic cancer using murine PanO2 cells.[14]

Beyond inhibiting the polyamine biosynthetic enzymes, another approach is to target the amino acid pools from which the polyamines are derived. LAT-1/SLC3A2 (large neutral aminoacid transporter 1) is a heterodimer comprised of a light subunit (SLC7A5, aka LAT-1) and a heavy subunit (SLC3A2, Figure 1). This complex transports large neutral aminoacids such as leucine, phenylalanine and methionine into mammalian cells. L-Leucine is used not only for protein synthesis, but also serves as an intracellular signaling molecule, which can regulate cell growth via stimulation of mTOR. Once activated, mTOR directly phosphorylates initiation factor 4E binding protein (4E-BP1) and p70 ribosomal S6 kinase 1 (p70S6K) to facilitate growth.[15] Activation of the mTOR pathway is found in many types of cancers and inhibitors of LAT-1 mediated transport (**5-8**) have been proposed as another anti-cancer strategy.[15] Indeed, inhibition of LAT-1 has been shown to suppress leucine uptake, mTOR signaling, and the growth of Panc-1 pancreatic cancer cells in vitro.[15]

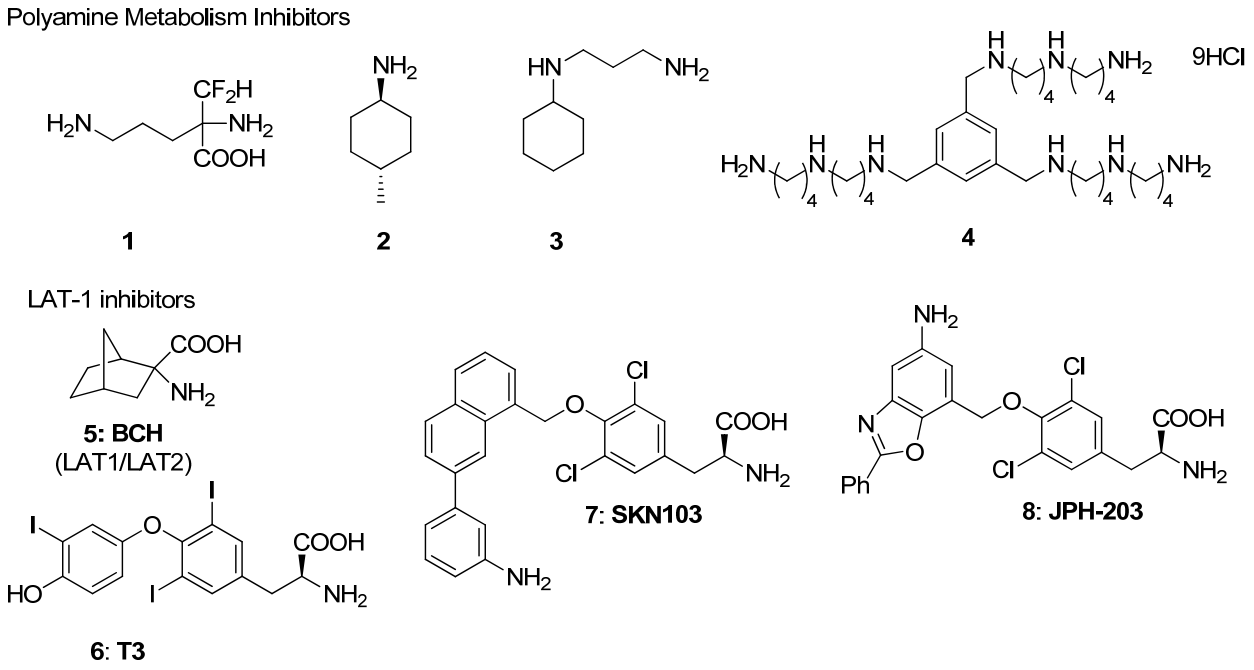

Figure 2. Current inhibitors of polyamine metabolism (**1-3**), polyamine import (**4**) and LAT-1 (**5-8**).

In a search for compounds which decrease intracellular polyamine levels, we screened several complex molecular libraries from the Torrey Pines Institute for Molecular Studies (TPIMS) and identified a lead architecture **A** for further investigation (Figure 3). This screen involved testing compounds generated at TPIMS for their ability to affect Chinese hamster ovary (CHO) cell growth in the presence of compounds that target polyamine metabolism and import. Originally designed to screen for PTIs, this assay serendipitously also identified compounds which affected polyamine pools and growth by other mechanisms. In a subsequent study of 250 individual compounds, we identified two promising hits (**9** and **10** in Figure 3). This report describes the synthesis and bioevaluation of these hit compounds, which appear to be efflux agonists of LAT-1 substrates (e.g., methionine and leucine).

L3.6pl pancreatic cancer cells treated in vitro with compound **10** (5 μM) were shown to have significantly higher levels of glutamic acid, agmatine (a derivative of arginine), leucine,

methionine, and phenylalanine, and ornithine in the supernatant and have significantly decreased intracellular leucine, methionine, spermidine and spermine pools compared to an untreated control. In summary, this work is significant as it provides a new way to reduce intracellular levels of hydrophobic aminoacids. In one example, methionine restriction induced by **10** depletes intracellular polyamine pools and reduces cell growth.

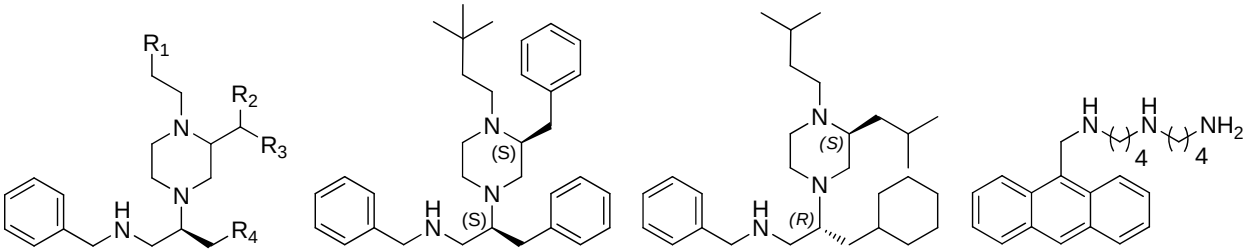

A **9** **10** **11: Ant-44** (3 HCl)

Figure 3. Lead architecture (**A**) identified from molecular library screening, top hits **9** and **10**, and **11** (**Ant-44**, a fluorescent cytotoxic polyamine).

Results and Discussion

Synthesis. Since the original TPIMS molecular libraries were synthesized via solid-phase peptide chemistry[16] to provide small quantities for screening purposes, we developed a solution phase synthetic approach to provide larger quantities of the top hits for further evaluation.

As a quick overview, our strategy (shown in Scheme 1 for compound **9**) involved several peptide coupling steps with HATU (1-[Bis(dimethylamino)methylene]-1*H*-1,2,3-triazolo[4,5-*b*]pyridinium-3-oxide hexafluoro-phosphate) to create a linear triamide scaffold **17** with the appropriate substituents. This triamide scaffold was then reduced with borane-THF to afford the respective chiral triamine **18**. Regioselective *N*-benzoylation of the terminal amine with *N*-hydroxysuccinimide ester **19** provided a diamine scaffold **20**, which could then be regiospecifically

cyclized with oxalyl diimidazole to form diketopiperazine **21.** Lastly, **21** could be reduced with BH_3/THF to form the desired target **9**.

As an example, the synthesis of compound **9** is shown in Scheme 1. The starting materials 3,3-dimethyl-butyric acid **12** and *L*-phenylalanine methyl ester hydrochloride **13** were used in the initial coupling step to form amide **14** (95%), which was then hydrolyzed to form carboxylic acid **15** (99% yield). HATU-mediated coupling of acid **15** to *L*-phenylalanine amide **16** gave triamide **17** albeit in low yield (39%). Reduction of the triamide using BH_3/THF provided the triamine **18** (52%). Subsequent *N*-benzoylation with *N*-hydroxysuccinimide ester of benzoic acid **19** gave the desired benzamide **20** in 90% yield. Cyclization of **20** with oxalyl diimidazole provided the diketopiperazine **21** (79% yield), which was reduced with BH_3/THF to give the desired compound **9** (65% yield). Overall, compound **9** was made in 9% yield over 7 steps.

Scheme 1[a]

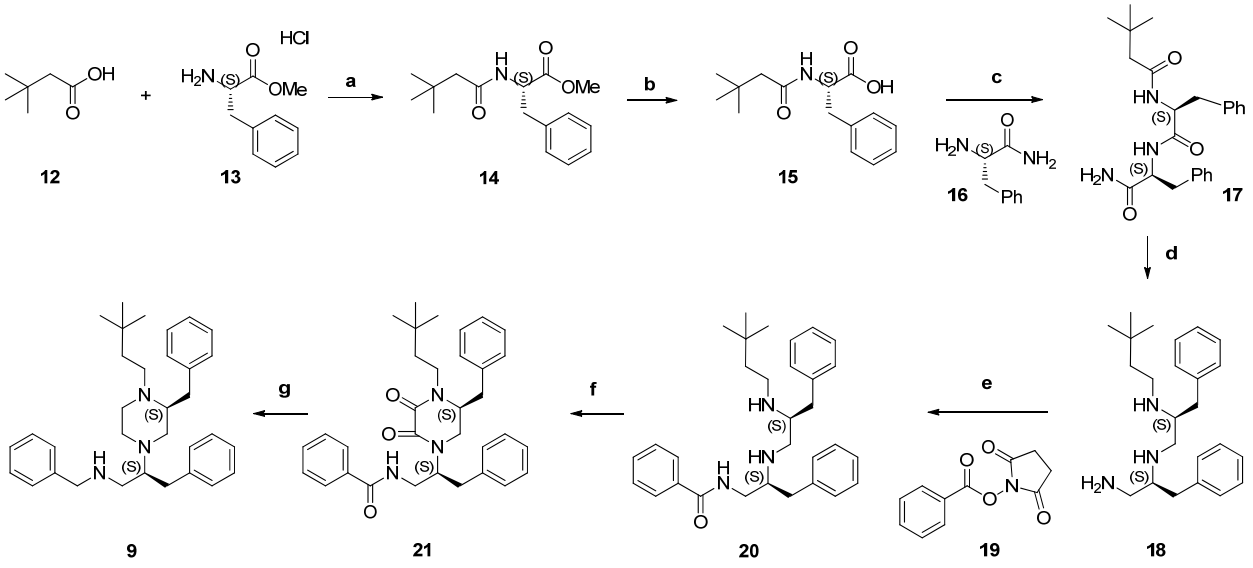

[a]*Reagents*: a) HATU, DIEA, DCM, rt, 95% yield; b) NaOH, MeOH, rt, 99% yield; c) HATU, DIEA, DCM, rt, 39% yield; d) BH_3-THF, THF, reflux, 52% yield; e) DCM, rt, 90% yield; f) oxalyl diimidazole (5 equiv), DCM, rt, 79% yield; g) BH_3-THF, THF, reflux, 65% yield

Compound **10** was synthesized using a modified approach to increase yield. As shown in Scheme 2, isovaleric acid **22** and *L*-leucine ether ester hydrochloride **23** were coupled via HATU to form amide **24** as the initial step in the synthesis of **10**. Amidoester **24** was then converted to the carboxylic acid **25** in 88% yield. To avoid the low yields encountered in the prior coupling of acid **15** with amide **16**, we first coupled acid **25** to *D*-cyclohexylalanine methyl ester **26** to give diamidoester **27** in 96% yield. Ammonia gas was used to convert the diamidoester **27** to triamide **28** in 82% yield. Note: this alternate approach to triamide formation (e.g., **28**) was a significant improvement over the related approach used to make triamide **17** in Scheme 1. The remainder of the synthesis was carried out as described above to give the target compound **10** in 22% overall yield after 8 steps. Note: the chiral integrity of the synthetic approach was maintained as evidenced by comparison of the circular diichroism spectrum of **10** to its three diastereomers, which were independently synthesized and will be reported in future work.

Scheme 2[a]

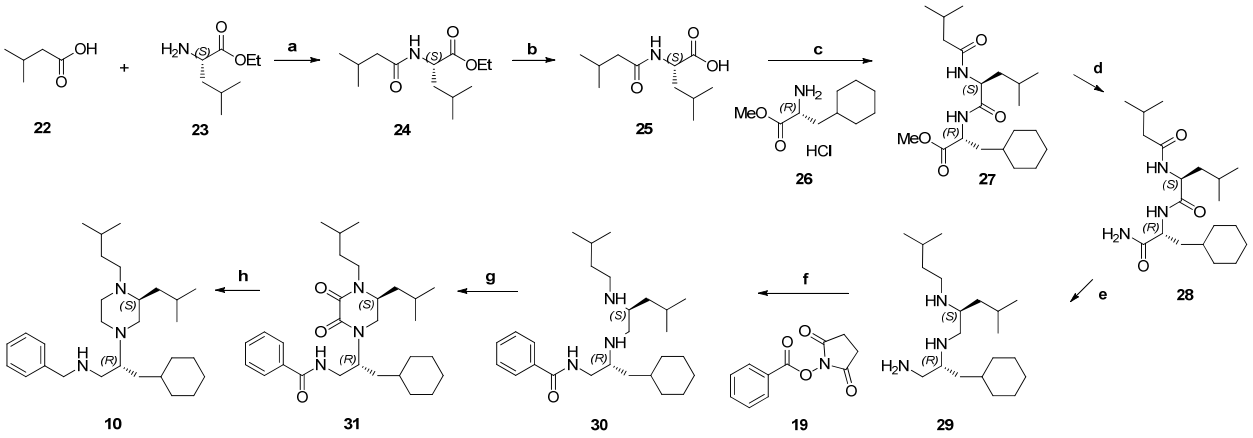

[a]*Reagents*: a) HATU, DIEA, DCM, rt, 93% yield; b) NaOH, MeOH, rt, 88% yield; c) HATU, DIEA, DCM, rt, 96% yield; d) NH_3 (*g*), MeOH, rt, 82% yield; e) BH_3-THF, THF, reflux, 97% yield; f) DCM, rt, 73% yield; g) oxalyl diimidazole (5 equiv), DCM, rt, 82% yield; h) BH_3-THF, THF, reflux, 60% yield

The bioevaluation of these compounds was then conducted using a series of assays designed to compare the ability of each compound to target polyamine metabolism and influence the transport of key amino acids and polyamines.

We first explored the ability of these polyamine-depleting compounds to affect polyamine transport using established assays in our laboratory.

CHO K1 Studies. Wild type Chinese hamster ovary (CHO K1) cells were chosen to first study the synthetic compounds' impact on polyamine metabolism. The CHO K1 cell line has high polyamine transport activity and was useful in screening the compounds for polyamine transport inhibition. A dose-response curve was obtained for each compound to determine their toxicity in CHO K1 cells after 48 h incubation. Compound **9** was non-toxic up to the highest dose tested (10

μM, see Figure S3). In contrast, compound **10** could be dosed for 48h up to 6 μM in CHO-K1 cells without apparent impact on cell growth (Figure S3).

Inhibition of ODC by DFMO often leads to an increase in polyamine transport activity to maintain intracellular polyamine homeostasis (Figure 1). The increased transport activity of DFMO-treated cells was used to assess the PTI activity of these compounds by investigating the ability of each compound to block the entry of a rescuing dose of spermidine (1 μM).[17-18] Our group has previously determined the 48 h IC_{50} value of DFMO in CHO K1 cells as 4.2 mM, as well as the minimum amount of spermidine (Spd, 1μM) required to rescue the DFMO-treated CHO K1 cells back to >90% viability.[7] These two parameters (4.2 mM DFMO and 1 μM Spd) remained fixed throughout the assay. The third parameter was the candidate PTI compound which was used in increasing doses up to its maximum tolerated concentration, MTC. The MTC is the maximum dose the compound could be dosed individually and provide >90% cell growth relative to an untreated control. Since non-toxic PTIs are expected to inhibit Spd entry, the cells treated with a combination of DFMO, Spd, and PTI would be expected to resemble the DFMO-only treated control. This assay allowed the potential PTIs to be tested, ranked, and compared.

In a 96-well plate format, CHO K1 cells were treated with the IC_{50} of DFMO (4.2 mM), a fixed dose of Spd (1 μM), and increasing doses of the potential PTI compounds. The cells were incubated for 48 h at 37°C. Results for compounds **9** and **10** are shown in Figure 4. The green line in Figure 4 represents the % relative growth observed with the DFMO+Spd control, while the red line represents the % relative growth for the DFMO-only control. The EC_{50} value is typically defined here as the concentration of the compound needed to reduce the % relative growth to halfway between the green and red lines, i.e. halfway between the DFMO+Spd and DFMO only controls. Interestingly, neither of the compounds (**9** or **10**) successfully blocked the entry of the

rescuing dose of Spd to the DFMO-treated CHO K1 cells and the EC_{50} could not be determined. In summary, these CHO K1 experiments demonstrated that compounds **9** and **10** did not act as effective PTIs in this cell line.

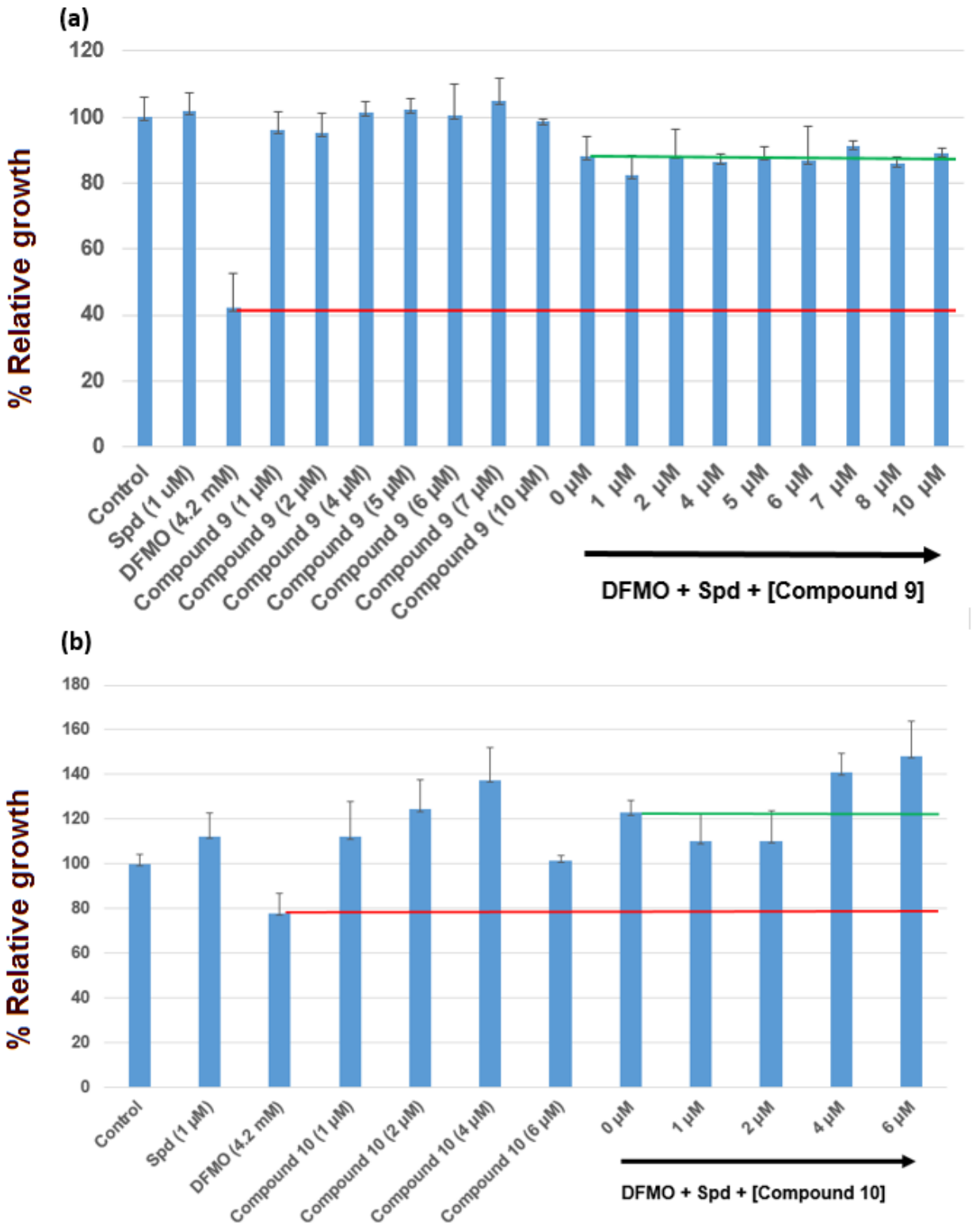

Figure 4. Inability of (a) Compound **9** and (b) Compound **10** to prevent Spd from rescuing DFMO-

treated CHO K1 cells. CHO K1 cells (1000 cells/well) were incubated at 37°C for 48 h in the presence of increasing doses of the respective compound in the presence of a fixed concentration of DFMO (4.2 mM) and Spd (1 μM). The cells were pre-incubated with 1 mM aminoguanidine (AG) for 24 h prior to compound addition. Column 1 shows the untreated CHO K1 control, while columns 2-10 in Panel A and columns 2-7 in Panel B show the % relative cell growth when the cells are dosed with either Spd (1 uM), DFMO (4.2 mM), or the compound alone at the different concentrations. The remaining columns in each panel are % relative cell growth in the presence of fixed concentrations of DFMO (4.2 mM) and Spd (1 μM) with increasing concentrations of the compounds indicated in each panel. Performance differences by DFMO were due to the presence of DMSO (0.15% by vol) used to dissolve compound **9** (Panel A), whereas compound **10** was dissolved in PBS (Panel B). The data suggests that neither compound is toxic in this dose range and neither performs as a PTI. Experiments were twice performed in triplicate and error bars show the standard deviation from the mean for each experiment.

To further assess PTI activity, we also screened the candidate compounds (**9** and **10**) for their ability to block Ant-44 entry (compound **11**). Ant-44 is a cytotoxic homospermidine, a anthracene-polyamine conjugate, previously synthesized in our lab.[19] Ant-44 is taken up into CHO K1 cells through the polyamine transport system (PTS). The selectivity for the PTS was demonstrated through IC_{50} comparisons between the CHO cell line and a mutant CHO cell line (CHO-MG). The CHO-MG cell line is a polyamine-transport-deficient cell line and represented cells with low PTS activity. Ant-44 displayed a nearly 150-fold preference for the CHO cell line over the CHO-MG, suggesting that Ant-44 has high affinity for targeting cells with active polyamine transport activity.[19] Additionally, we have previously shown that the presence of

exogenous spermidine provides cell protection from the polyamine conjugate Ant-44 by spermidine's competitive access to cells via the PTS.[20] Based on this result, we concluded that a PTI, especially a polyamine-based PTI like compound **4** in Figure 2, would also block Ant-44 uptake.

We envisioned that a non-toxic PTI would inhibit the uptake of the cytotoxic polyamine conjugate Ant-44 (**11**) and rescue cells from Ant-44 associated toxicity. For example, using the IC_{50} dose of Ant-44, PTIs could be identified by measuring a compound's ability to block Ant-44 entry and rescue cells back to >90% relative cell growth. Previous studies demonstrated that Ant-44 (2.4 μM) significantly reduced cell viability in CHO K1 cells after 48 h incubation. This toxic dose of Ant-44 was kept constant throughout the assay, while the candidate PTI was added in increasing concentrations up to its MTC.

CHO K1 cells were treated in a 96-well plate with a toxic dose of Ant-44 (2.4 μM) alone and dosed with the candidate compounds (**9** and **10** at the non-toxic doses of 5 μM and 7 μM) and incubated for 48 h at 37°C. Compounds **9** and **10** exhibited intriguing activity. Rather than rescue the cells from Ant-44, the compounds seemed to significantly potentiate Ant-44's toxicity. For example, Ant-44 alone (2.4 μM) gave 23% relative cell growth, whereas Ant-44 in combination with compounds **9** or **10** at 7 μM gave significantly reduced relative cell growth at 2.1% and 3%, respectively, compared to the untreated control. Since neither **9** or **10** was toxic below 7 μM in CHO K1 cells (Figure S3), this result implied potential synergism between these compounds and Ant-44. At this point, our PTI discovery work flow was disrupted because we had identified new structures, which gave the opposite result than expected.

To further explore this novel effect, we modified our original screen to use a lower dose of Ant-44 (0.5 μM) to improve the dose range of **9** and **10** that could be tested. In this regard, Ant-44 was dosed at 0.5 μM alone and in combination with increasing doses of compounds **9** and **10** up to 5 μM. The CHO K1 cells were incubated for 48 h at 37°C, and the results are shown in Figure 5. The red line represents the % relative cell growth of the Ant-44 only control. The Ant44 potentiation assay EC_{50} value is defined as the concentration of the candidate compound required to decrease the cell growth to half that of the Ant-44 only control. Both compounds **9** and **10** were effective at decreasing cell growth, when used in combination with Ant-44 in a dose-dependent fashion. Additionally, compounds **9** and **10** exhibited very low EC_{50} concentrations in CHO cells in the presence of Ant-44 (0.5 μM), with EC_{50} values of 750 nM and 60 nM, respectively. We noted that compound **10** was approximately 12.5 times more effective at potentiating Ant-44 than compound **9** in CHO K1 cells.

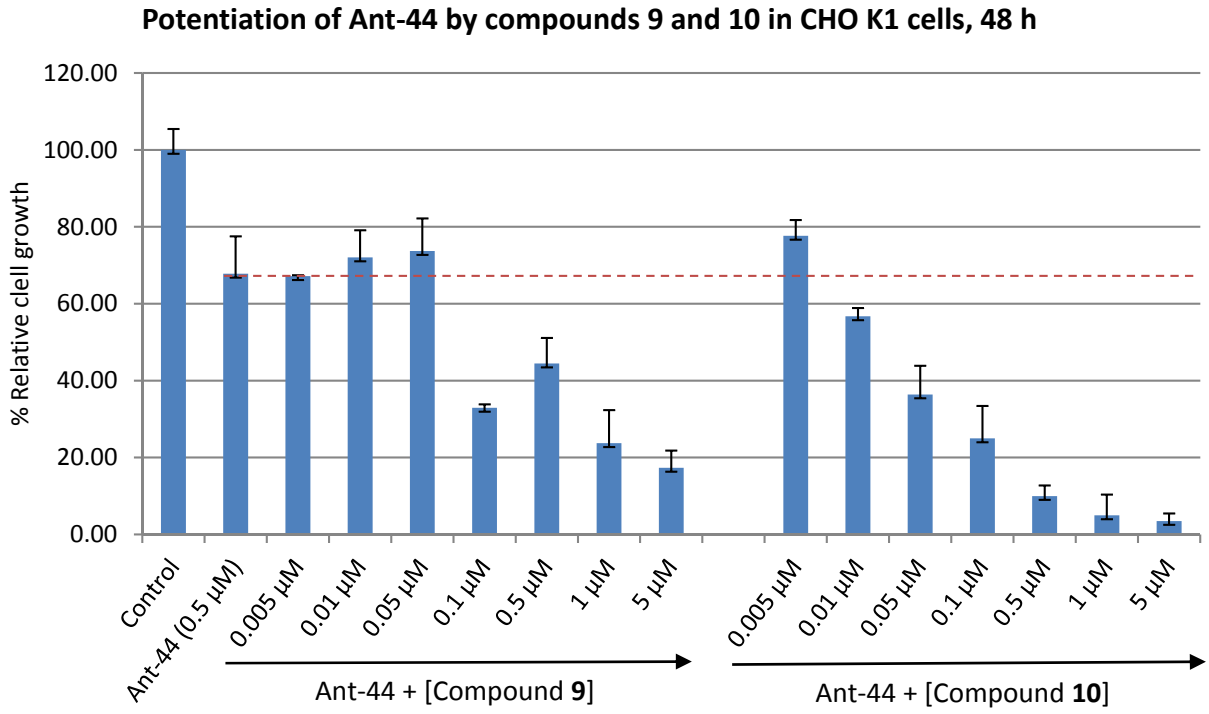

Figure 5. Potentiation of Ant-44 toxicity by compounds **9** and **10** in CHO K1 cells. CHO K1 cells were incubated for 48 h at 37°C with the respective compound and a fixed concentration of cytotoxic Ant-44 (0.5 µM). Aminoguanidine (AG, 1 mM) solution was incubated with the CHO K1 cells for 24 h prior to the addition of candidate compound. This was necessary to protect Ant-44 from the amine oxidases present in the media containing fetal bovine serum. Column 1 is the untreated CHO K1 control cells, column 2 shows the % relative cell growth (compared to the untreated control) when dosed with Ant-44 alone at 0.5 µM, columns 3-16 have a fixed concentration of Ant-44 (0.5 µM) with increasing concentrations of the candidate compounds as indicated in each lane. Both compounds **9** and **10** are non-toxic to CHOK1 cells at the highest concentration tested (5 µM). The Ant-44 potentiation EC_{50} values, defined as the concentration to reduce the viability to half the Ant-44 only control, were 0.75 µM (**9**) and 0.06 µM (**10**),

respectively. Experiments were twice performed in triplicate and error bars show the standard deviation from the mean for each experiment.

To observe changes to the cell as a result of treatment with these compounds, the control CHO K1 cells and the cells treated with Ant-44 (0.5 μM) and compound **10** at 5 μM in the aforementioned 96-well plate experiment were observed under the microscope. As shown in Supporting Information (Figure S1), the treated cells were not ruptured, and differed from the control in terms of their number and rounded shape (in comparison to the more elongated control cells). This data suggested that the treated cells were not growing. Intrigued by these observations, we investigated the properties of these compounds in the L3.6pl human pancreatic cancer cell line.

L3.6pl Studies. Compounds **9** and **10** were evaluated in the metastatic human pancreatic cancer cell line, L3.6pl. L3.6pl cells have a K-*ras* mutation, and high polyamine uptake activity.[7] A dose-response curve was obtained for each compound in L3.6pl cells to determine the 72h L3.6pl IC_{50} value, defined as the dose at which L3.6pl cells gave 50% relative growth compared to the untreated control. Compounds **9** and **10** had 72h IC_{50} values of 11.7 ± 0.9 μM and 5.9 ± 0.2 μM, respectively. We noted that compounds **9** and **10** were more toxic to L3.6pl cells compared to CHO K1 cells.

As performed previously with CHO K1 cells, L3.6pl cells were treated with compounds **9** and **10** and a fixed dose of Ant-44 to observe the potentiation effect. The 72 h IC_{50} dose of Ant-44 in L3.6pl cells was previously determined by our group to be 4 μM. For this study, we used half that dose to replicate the large 'window' of response used in the CHO experiments to look at reduction in cell growth. In a 96-well plate, L3.6pl cells were dosed with a fixed concentration of

Ant-44 (2 μM) and increasing doses of compounds **9** and **10**. The cells were incubated for 72 h at 37°C, and the results are shown in Figure 6. Although both compounds were effective at reducing cell growth, higher doses were required compared to CHO K1 cells. The EC_{50} for compound **9** was 3.27 ± 0.17 μM and compound **10** was 0.29 ± 0.1 μM. Both compounds were effective well below their 72 h IC_{50} dose in L3.6pl cells. Similar to our observations in CHO K1 cells, compound **10** was approximately eleven times more effective at increasing the potency of Ant-44 in L3.6pl cells than compound **9**.

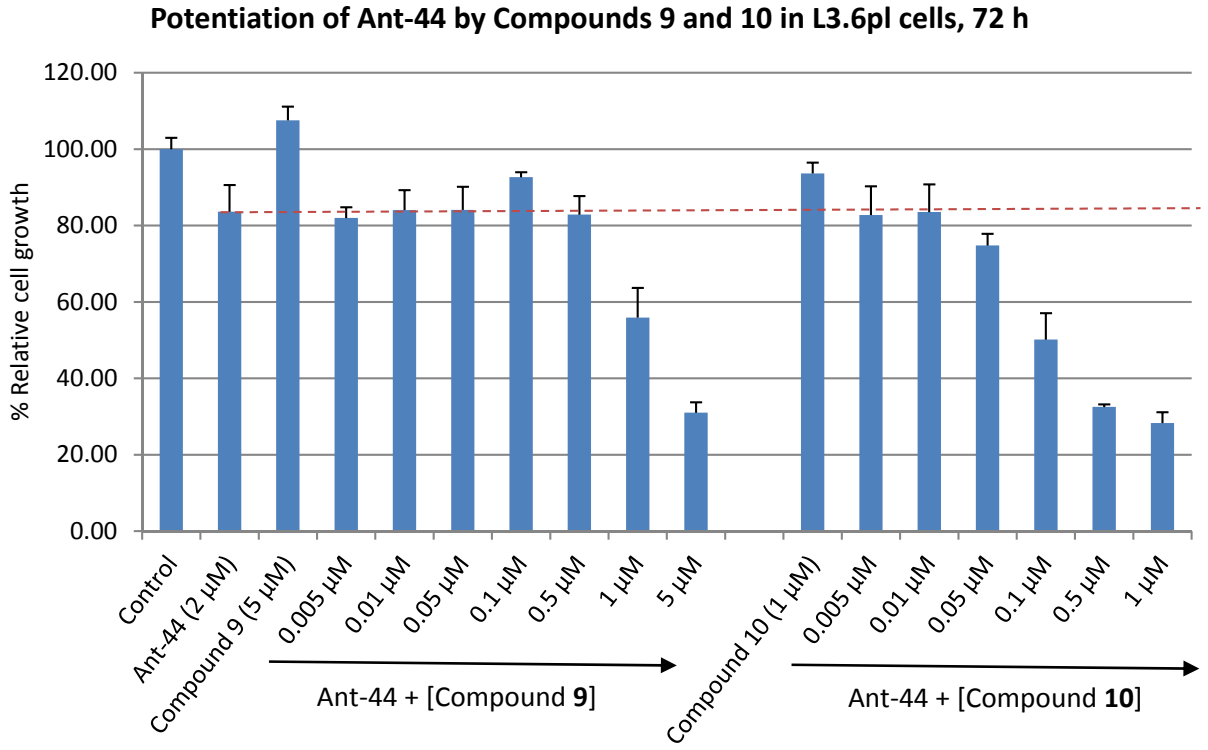

Figure 6. Ability of compounds **9** and **10** to potentiate the effect of Ant-44 in L3.6pl cells. Cells were incubated for 72 h at 37°C with the respective compound and Ant-44 (2 μM). A solution of AG (250 μM) in phosphate buffered saline (PBS) was incubated with the cells for 24 h prior to addition of compounds. Column 1 is the untreated L3.6pl control cells, column 2 shows the % cell viability when dosed with Ant-44 alone at 2 μM, columns 3-16 have a fixed concentration of

Ant-44 (2 μM) with increasing concentrations of the candidate compounds as indicated in each lane. Note: compounds **9** and **10** were nontoxic when tested alone at 5 μM and 1 μM, respectively.

To understand why Ant-44 becomes more potent in the presence of these compounds, especially in the presence of compound **10**, we designed an experiment to relate inhibition of cell growth to intracellular polyamine and Ant-44 levels. One explanation for the enhanced potency was that compound **10** increased polyamine import and, as a result, may have increased intracellular Ant-44 levels. To test this hypothesis, we dosed L3.6pl cells with a fixed concentration of Ant-44 (2 μM) alone and in combination with increasing concentrations of compound **10** to explore how this combination therapy affected intracellular polyamine pools and Ant-44 import. These results are displayed in Figure 7.

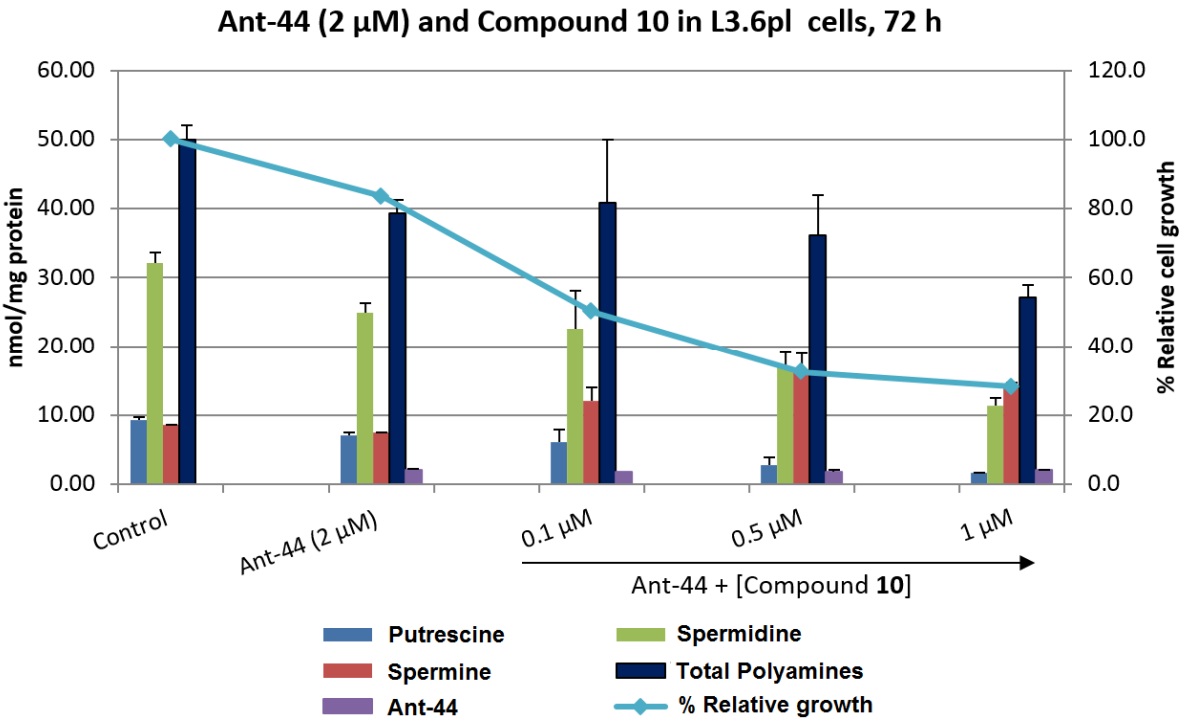

Figure 7. Single and combination therapies in L3.6pl cells with Ant-44 and compound **10** after 72h incubation. Polyamine and Ant-44 levels (expressed as nmoles/mg protein) and relative % cell growth versus an untreated control were observed after 72 h incubation at 37°C. The untreated control was run in parallel and polyamine levels determined in duplicate and % cell growth in triplicate. Ant-44 was dosed at a fixed concentration of 2 µM and compound **10** at increasing concentrations. Cell viability tracked well with total intracellular polyamine levels (sum of putrescine, spermidine and spermine).

Neither Ant-44 (2 µM) or compound **10** at 1 µM alone significantly reduced cell growth as measured by the MTS assay. The intracellular level of Ant-44 was essentially unchanged, where

the Ant-44 only control gave 2.15 ± 0.10 nmol Ant44/mg protein and when compound **10** at 1 μM was present at 2.08 ± 0.05 nmol Ant-44/mg protein. If compound **10** was acting as a polyamine import agonist, then we would expect the level of Ant-44 in the cells to increase with increasing doses of compound **10.** However, this was not observed.

Since compound **10** was neither acting as a PTI nor as a polyamine import agonist, how could it lead to intracellular polyamine depletion? The decreased levels of intracellular polyamines (putrescine, spermidine, and spermine) when L3.6pl cells are dosed with Ant-44 in combination with compound **10** at 1 μM suggested that compound **10** may act via a different mechanism. To test this hypothesis, we dosed L3.6pl cells with increasing concentrations of compound **10** without Ant44. If compound **10** was acting on polyamine pools, one should see a reduction in total polyamine levels as well as decreased cell viability in a dose dependent manner upon increasing levels of **10**. Therefore, we determined the toxicity of compound **10** by itself over a time range (24, 48, and 72h exposure, Figure S2 in Supporting Information) and measured intracellular polyamine levels after 72h exposure to **10** (Figure 8). The results of these latter experiments are shown in Figure 8.

Compound **10** demonstrated increasing toxicity to L3.6pl cells over extended periods of incubation (24, 48, and 72h, Figure S2). As shown in Figure 8, after 72h of incubation of L3.6pl cells with **10** at 37^{o}C, the intracellular polyamine levels of spermidine and spermine were significantly reduced, whereas the putrescine content was relatively unaffected.

This was interesting because typically another polyamine depletion approach (DFMO+PTI treatment) led to an absence of putrescine and a significant reduction in spermidine pools, while the spermine pools were maintained (or even increased). We recently performed a systematic

study of polyamine biosynthesis inhibitors (using DFMO, MCHA and CDAP) in L3.6pl cells and revealed the plasticity of polyamine homeostasis in these pancreatic cancer cells. The cells maintained viability as long as either the spermine or spermidine pools were maintained near basal levels and as long as the total polyamine pools were ≥ 40% of the untreated control. This suggested that these cells maintain an excess pool of polyamines to help offset changes in intracellular polyamine levels. For example, L3.6pl cells displayed 100% relative growth compared to an untreated control in the presence of the SMS inhibitor (CDAP, 100 μM) and had no detectable spermine.[10] Since compound **10** gave specific depletion of both spermidine and spermine pools (Figure 8), we speculated that it works through a different mechanism than DFMO+PTI.

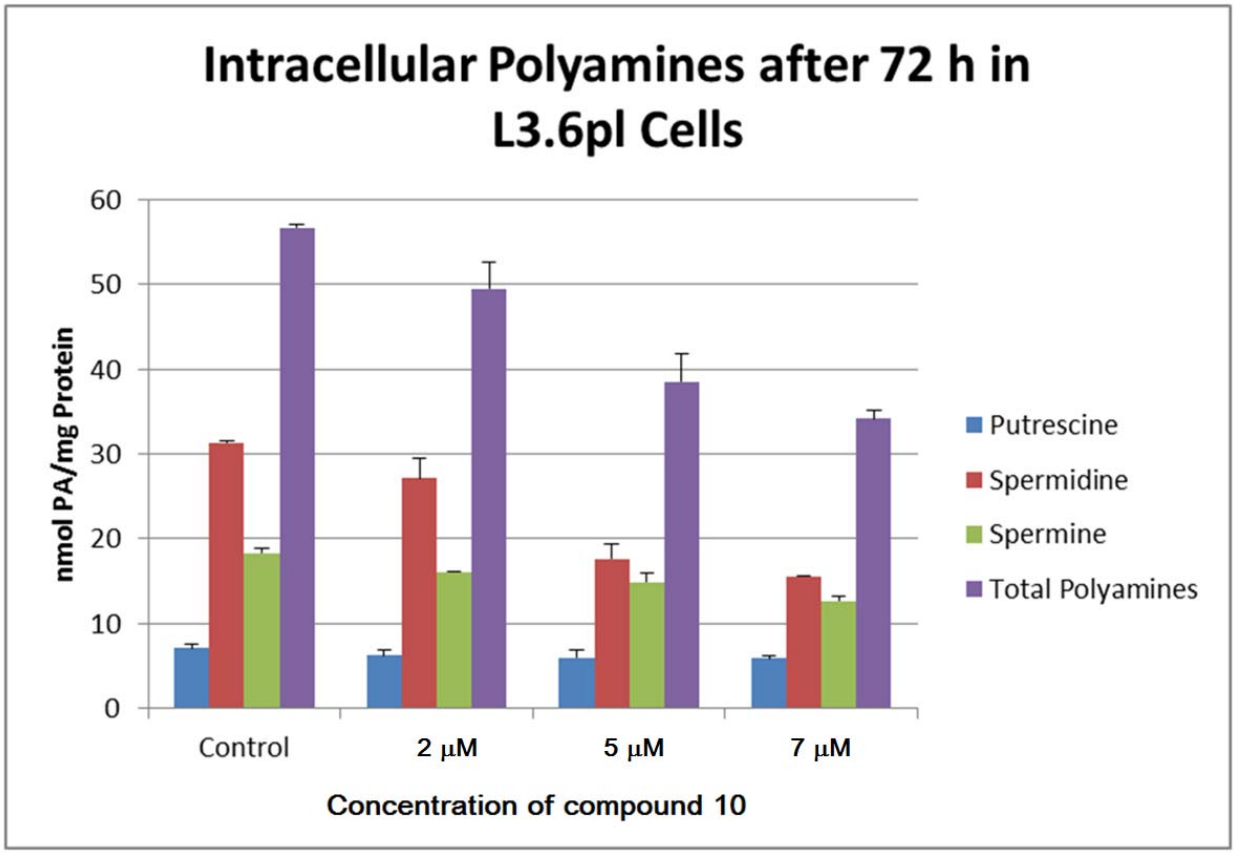

Figure 8. Intracellular polyamine levels (expressed as nmoles polyamine/mg protein) in L3.6pl cells dosed with increasing concentrations of compound **10** after cells were incubated for 72 h at

37°C. The untreated control was run in parallel and polyamine levels determined in duplicate via *N*-dansylation and HPLC. The data was averaged and reported as nmol polyamine (PA)/mg protein.

For example, DFMO+PTI treated L3.6pl cells were shown to have no detectable putrescine.[7] As shown in Figure 8, however, putrescine levels were relatively untouched (83% remaining) by compound **10** (7 μM) compared to the untreated control. Why then do these cells lose 50% of their spermidine pools and 30% of their spermine pools in the presence of compound **10**?

One way to affect both spermidine and spermine pools is to inhibit methionine import, which in turn would inhibit the formation of the decarboxylated S-adenosylmethionine needed to provide the aminopropyl fragment required for spermidine and spermine synthesis. Since methionine, leucine and phenylalanine all use the LAT1/SLC3A2 transporter to enter cells, we hypothesized that **10** was inhibiting LAT mediated amino acid import.

To test this hypothesis, we measured the amino acid concentrations in the supernatants of L3.6pl cells incubated with compound **10** at 2 μM and 5 μM for 72h compared to an untreated control (0 μM). This was straightforward to perform as these cells are adherent and one can directly sample the supernatant. Even though the cells were all plated initially at the same cell density, some conditions were toxic to the cells and reduced the number of cells available to metabolize amino acids in the media. We controlled for this feature by first sampling the supernatant and then harvesting the attached cell population. The harvested cells were washed, counted, and then lysed open to obtain samples of their intracellular contents. The remaining cell pellet after lysis was quantified for protein content (see Experimental section) to provide the mg of protein associated

with each sample. The results are shown in Table 1 and are expressed as pmol of analyte/mg protein in an effort to account for changes in cell population over the course of the experiment.

Table 1. Concentration (pmoles/mg protein) of specific metabolites collected in the supernatant of L3.6pl cells grown for 72h at 37°C in the presence of increasing doses of compound **10**[a]

Compd **10**	**Putrescine**	**Spermidine**	**Acetyl spermidine**	**Spermine**	**Acetyl spermine**	**Glutamic acid**
0 μM	977 ± 522	339 ± 340	1936 ± 1365	6152 ± 5596	77 ± 43	23412 ± 3983
2 μM	938 ± 70	131 ± 26	1649 ± 18	2532 ± 406	49 ± 10	20231 ± 649
5 μM	2224 ± 98	167 ± 32	1706 ± 29	2690 ± 889	36 ± 4	34033 ± 540

Compd **10**	**Agmatine**	**Arginine**	**Leucine**	**Methionine**	**Ornithine**	**Phenylalanine**
0 μM	101 ± 142	22121 ± 10585	18009 ± 9061	22834 ± 1984	10588 ± 3212	14299 ± 7194
2 μM	297 ± 163	18396 ± 70	15055 ± 1043	17686 ± 2432	9249 ± 306	11954 ± 828
5 μM	485 ± 176	43243 ± 2047	202092 ± 23817	64036 ± 5454	15951 ± 118	160462 ± 18910

[a] samples were run in duplicate.

As shown in Table 1, high levels of specific amino acids were observed in the presence of compound **10** (5 μM). The highest levels were observed with leucine (Leu), phenylalanine (Phe) and methionine (Met), i.e., the known LAT-1 substrates. Having gathered initial support for LAT as the potential target of **10**, we then determined the amount of Leu and Met remaining in cells after 72h incubation with compound **10**. These results are shown in Table 2.

Table 2. Intracellular concentrations after L3.6pl cell lysis (pmol/mg protein) after 72h incubation in the absence and presence of compound **10**[a]

Compound 10 (μM)	Leucine (pmol/mg protein)	Methionine (pmol/mg protein)
0	232 ± 10	167 ± 67
2	152 ± 8	226 ± 21
5	94 ± 3	41 ± 23
7	77 ± 1	Not detected

As shown in Table 2, a dose-dependent decrease in both leucine and methionine was observed. Taken together, Tables 1 and 2 suggested that compound **10** influences the transport of large neutral aminoacids and resulted in significant depletion of methionine and leucine pools in these cells.

LAT-1 is a known antiporter, wherein intracellular glutamine is exchanged with extracellular LAT-1 substrates like leucine and methionine. As a result of these data, we hypothesized that compound **10** may act as a LAT import inhibitor or as a LAT efflux agonist. We note that leucine and β-cyclohexylalanine (a reduced form of phenylalanine) are used in the synthesis of **10**. As a result, the molecular design of **10** (Figure 3) contains isobutyl and cyclohexylmethyl substituents which resemble the side chains of the natural substrates of LAT-1 (leucine and phenylalanine). We speculate that these features may provide **10** with special affinity for the hydrophobic recognition sites on LAT-1; an idea that will be pursued in future work. [21]

We note that virtually all known LAT-1 import inhibitors have amino acid motifs within their structure and have large hydrophobic side chains (see Figure 2).[22] In this regard, compound **10** provides a new scaffold for targeting LAT via a decorated piperazine motif. Instead of presenting a hydrophobic amino acid to LAT (see LAT1 inhibitors in Figure 2), compound **10** presents the

hydrophobic side-chains of the natural substrates (or mimics thereof) on a piperazine scaffold. We speculated that compound **10** may outcompete the native amino acids by presenting four of these recognized side chain 'arms' from a single platform. We note that this multi-prong substrate approach has worked in other import systems, where for example, a tri-substituted system outperformed a one- or two-armed system to more efficiently inhibit polyamine import.[7, 23]

Intrigued by these possibilities, we investigated potential mechanisms of action for how compound **10** depletes intracellular methionine and leucine stores. One possibility is that **10** inhibited the LAT-mediated uptake of these amino acids, so we investigated whether compound **10** inhibited the entry of exogenous ^{3}H-leucine into L3.6pl human pancreatic cancer cells. We elected to use ^{3}H-leucine for these uptake studies to conform to the published methods in this area. As shown in Figures 9-12, these results were compared to the known LAT-1 inhibitor, JPH-203.[24]

In control experiments run at two key temperatures, 4ºC (a condition where active transport is inhibited) vs. 37ºC (a temperature at which active transport occurs) in L3.6pl cells, we demonstrated that 60% of the bound ^{3}H leucine pool was actively transported into cells and 40% was tightly bound presumably to the outside of cells (and could not be washed off upon repeated washing steps with 4ºC buffer). This 40/60 ratio was determined by comparing the total radioactivity counts associated with the washed cell pellets of the 4ºC experiment and the 37ºC experiment. Note: In both experiments, the unbound ^{3}H-leucine was removed via three separate washing steps of the cells with 4ºC buffer. Having a good understanding of where the ^{3}H-labeled leucine partitioned during the assay and the source of background signals, we then verified the dose dependent decrease in the uptake of ^{3}H Leucine using the known LAT 1 inhibitor JPH-203 (Figure S3, Supporting Information). [24]

In contrast to JPH-203, compound **10** showed no inhibition of ^{3}H-leucine uptake over a 2 min incubation period. Other experiments were conducted including a longer pre-incubation period with **10** (24h) and washed cells (Figure 9, left) and a 24h pre-incubation with **10**, followed by a 30 min of incubation with **10** and ^{3}H-Leu (Figure 9, right). None of these experiments demonstrated inhibition of ^{3}H-Leu uptake by **10**.

To further confirm these results, we used an indirect measurement of leucine import via a trans-stimulation efflux assay. Trans-stimulation occurs when exogenous leucine is imported into cells and triggers the export of endogenous leucine. This leucine-for-leucine exchange requires the import of exogenous leucine into the cell. Indeed, using L3.6pl cells pre-loaded with ^{3}H-leucine (and washed), one can measure the efflux of ^{3}H-leucine stimulated by the presence (and import) of unlabeled leucine in the supernatant. A leucine uptake inhibitor, like JPH-203, would be expected to block the uptake of unlabeled leucine and, thus, inhibit the efflux of endogenous radiolabeled leucine. In contrast, a compound which did not block exogenous leucine uptake (i.e., compound **10**) would not be expected to inhibit the efflux of ^{3}H-leucine from inside the cell.

Briefly described, L3.6pl pancreatic cancer cells were preloaded for 5 min with ^{3}H-leucine ('hot' label) at 37^{o}C, then the unbound ^{3}H-leucine is washed away (three times) with cold Hanks' balanced salt solution (HBSS). These washed, preloaded 'hot' L3.6pl cells are then incubated for 2 minutes at 37^{o}C in the presence and absence of unlabeled leucine (100 μM). The unlabeled leucine enters cells (presumably via LAT1) and triggers the efflux of the preloaded ^{3}H-leucine into the supernatant, which is collected and the radioactivity measured. A LAT-1 inhibitor, like JPH-203, would be expected to block the entry of the unlabeled leucine and limit the efflux of the ^{3}H-leucine into the supernatant over the 2 min period. As shown in Figure 10, JPH-203 (at 30 μM) inhibited the efflux of ^{3}H-leucine as expected. In contrast, as shown in Figure 11, compound **10**

(either at 2 μM or 20 μM) did not inhibit the efflux of ^{3}H-leucine. Together, these result confirmed that compound **10** was neither able to inhibit leucine import nor inhibit the trans-stimulated export of leucine under these conditions. In sum, we have demonstrated by two different assays, both of which rely on leucine uptake, that **10** does not inhibit leucine uptake. How then does **10** cause intracellular leucine/methionine depletion, especially when there are ample supplies of leucine/methionine outside the cell as inferred by Table 1?

Another potential mechanism of action is via enhanced leucine/methionine efflux. A slow export of leucine and methionine stores would eventually result in significant intracellular depletion given enough time. This property would be missed in the above kinetic efflux experiments, which are completed in short time frames. Indeed, unlabeled leucine (at 100 μM) gives maximal trans-stimulated efflux after 2 min, which may have swamped the putative small efflux signal generated by compound **10**. A subsequent study showed that compound **10** alone increased efflux of ^{3}H-Leu albeit at higher doses (60 μM) and after a 30 min incubation time at 37^{o}C (shown in Figure 12). In this regard, our earlier experiments using 2 and 15 min incubation time periods and lower concentrations of **10** (<7 μM) were likely too short and too low in **10** to detect this slow efflux induction by **10** itself.

The exciting result here is that this amino acid depletion seems to occur even though there are significant levels of extracellular amino acids available to replenish the depleted cellular stores (*vide infra* from Tables 1 and 2). We speculate that since compound **10** does not appear to inhibit uptake of exogenous leucine (Figure 9), it likely induces an overall net loss of leucine (and methionine) via a 'slow leak' mechanism. In this scenario, the uptake of extracellular pools of LAT-1 substrates is unable to compensate for the overall efflux of these aminoacids from the cell. We speculated that since LAT-1 is a known antiporter of leucine and methionine, it is possible that

compound **10** is an efflux agonist of LAT-1. Importantly, as shown in Figure 12, the presence of the LAT-1 specific inhibitor, JPH-203, significantly inhibited the efflux induced by compound **10** suggesting that **10** is, indeed, targeting LAT-1 mediated efflux.

The fact that this phenomenon seems to affect hydrophobic aminoacids (leucine, methionine and phenylalanine) is also consistent with these findings. Tying these observations together, since methionine and leucine both use LAT-1, the hydrophobic amino acid efflux induced by **10** (Figure 12) likely depletes the levels of intracellular methionine (Table 2) and inhibits cellular processes, which rely upon methionine pools (e.g., spermidine and spermine biosynthesis, Figure 8).

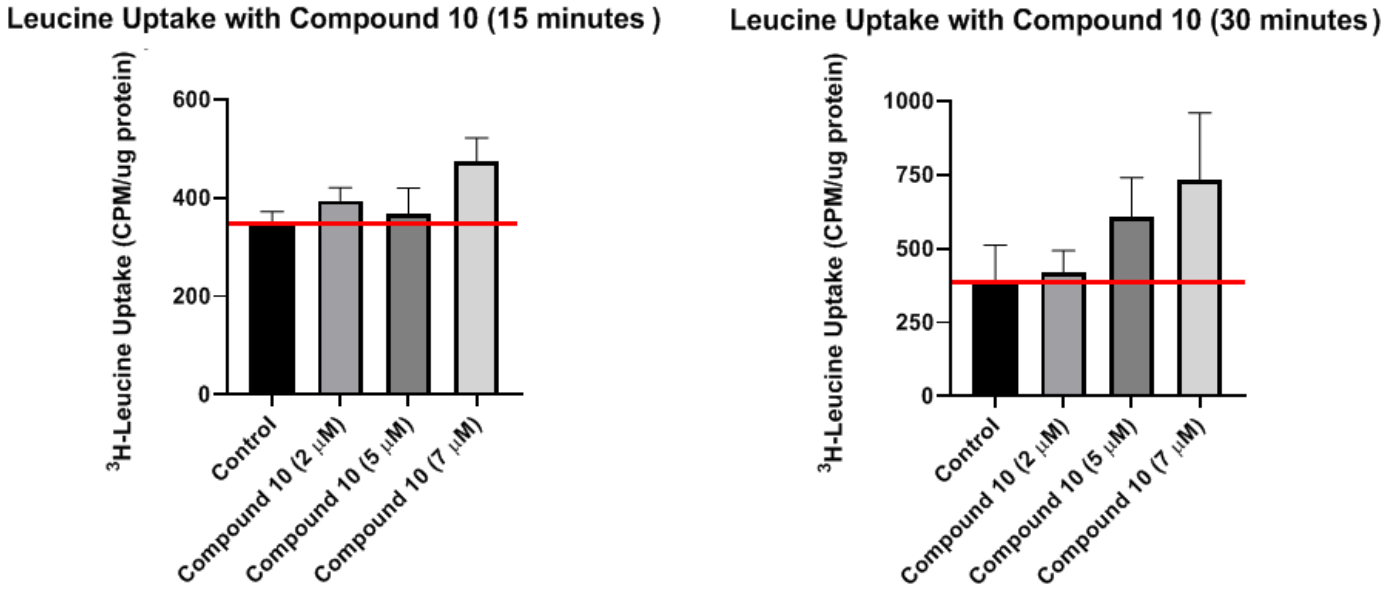

Figure 9. Several import inhibition scenarios were tested. First, leucine uptake experiments with L3.6pl cells incubated with compound **10** and ^{3}H-leucine for 2 minutes (vs. control) showed no inhibition of ^{3}H-Leu uptake (data not shown). Therefore, we looked at longer ^{3}H-Leu uptake times (15 and 30 min) and pre-incubated L3.6pl cells with compound **10** for 24h to give the molecule more time to reach its putative target. (Left panel): Leucine uptake inhibition experiments were conducted after L3.6pl cells were pre-incubated with compound **10** for 24 h at 37ºC (vs. control). In case 1, compound **10** was washed off, HBSS added, and ^{3}H-leucine uptake measured over 15 min at 37ºC with the washed L3.6pl cells. Values below the red line shown was considered due to inhibition of ^{3}H-Leucine uptake. We concluded that compound **10** did not inhibit ^{3}H-Leu uptake under these pre-incubation/washed cells condition. (Right panel): We repeated this experiment and pre-incubated L3.6pl cells with compound **10** for 24 h at 37ºC, washed the cells, HBSS was added, but this time added back **10** to the cells, just prior to adding the ^{3}H-leucine and incubating for 30 min at 37ºC. As shown in the right panel, no inhibition of ^{3}H-Leu was observed. The data was

normalized by dividing by µg of protein. In sum, none of these experiments demonstrated inhibition of ^{3}H Leu uptake by compound **10**.

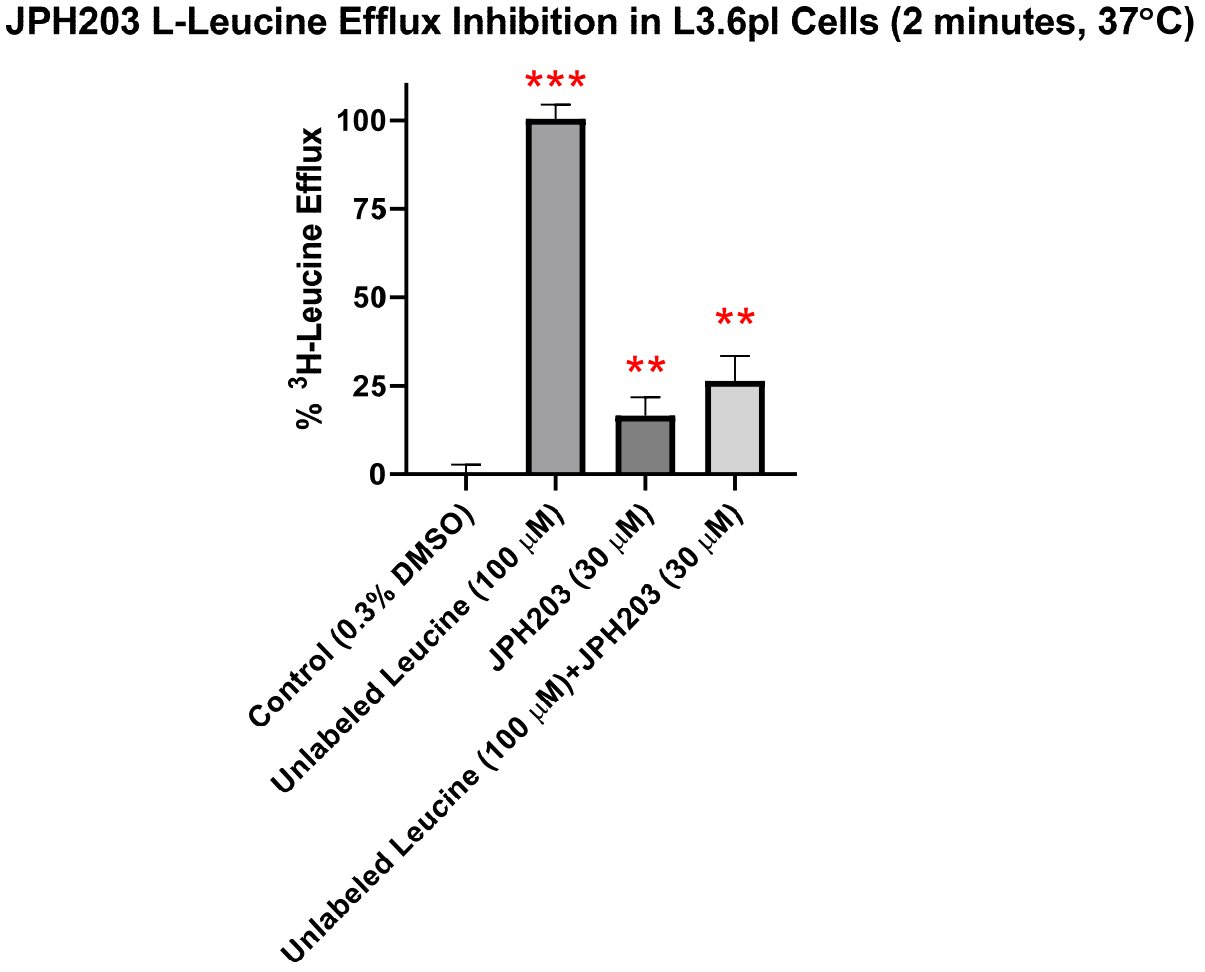

Figure 10. *^{3}H Leucine efflux from L3.6pl cells through trans-stimulation with unlabeled leucine (100 µM) in the presence and absence of JPH-203 at 30 µM after 2 min incubation at 37°C.* As shown in the rightmost column, JPH-203 significantly inhibited efflux of ^{3}H-leucine due to its ability to inhibit the uptake of unlabeled leucine into the cell. Asterisks: ** $p<0.01$; *** $p<0.001$ via Student t-test.

A **L-Leucine Efflux Inhibition in L3.6pl Cells (2 minutes, 37°C)**

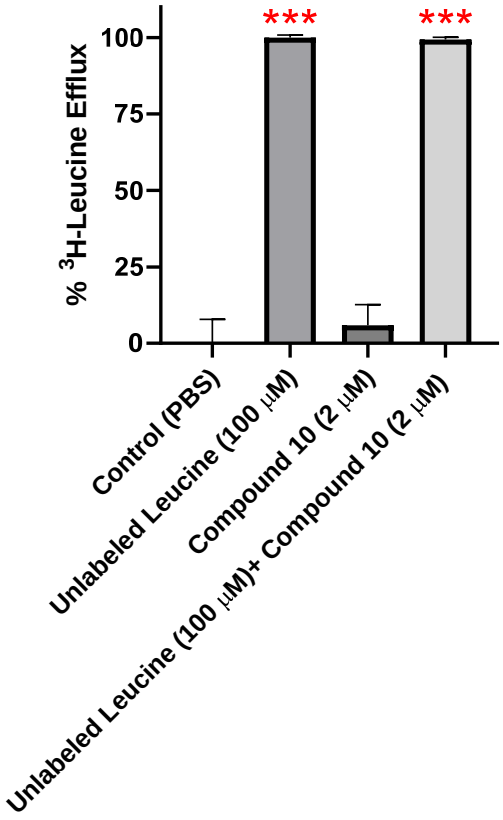

B **L-Leucine Efflux Inhibition in L3.6pl Cells (2 minutes, 37°C)**

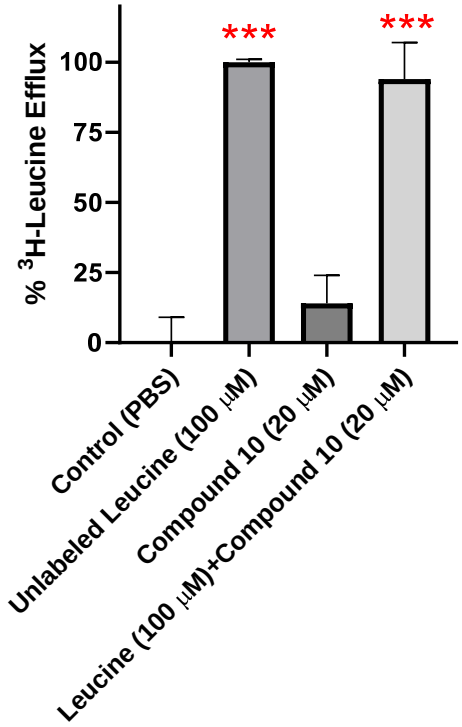

Figure 11. *^{3}H Leucine efflux from L3.6pl cells through trans-stimulation with unlabeled leucine (100 μM) in the presence and absence of compound **10** at either 2* or 20 *μM after 2 min incubation at 37°C.* Compound **10** did not inhibit efflux of ^{3}H-leucine at either concentration likely due to its inability to block the uptake of unlabeled leucine into the cell. Asterisks: *** $p<0.001$ via Student t-test.

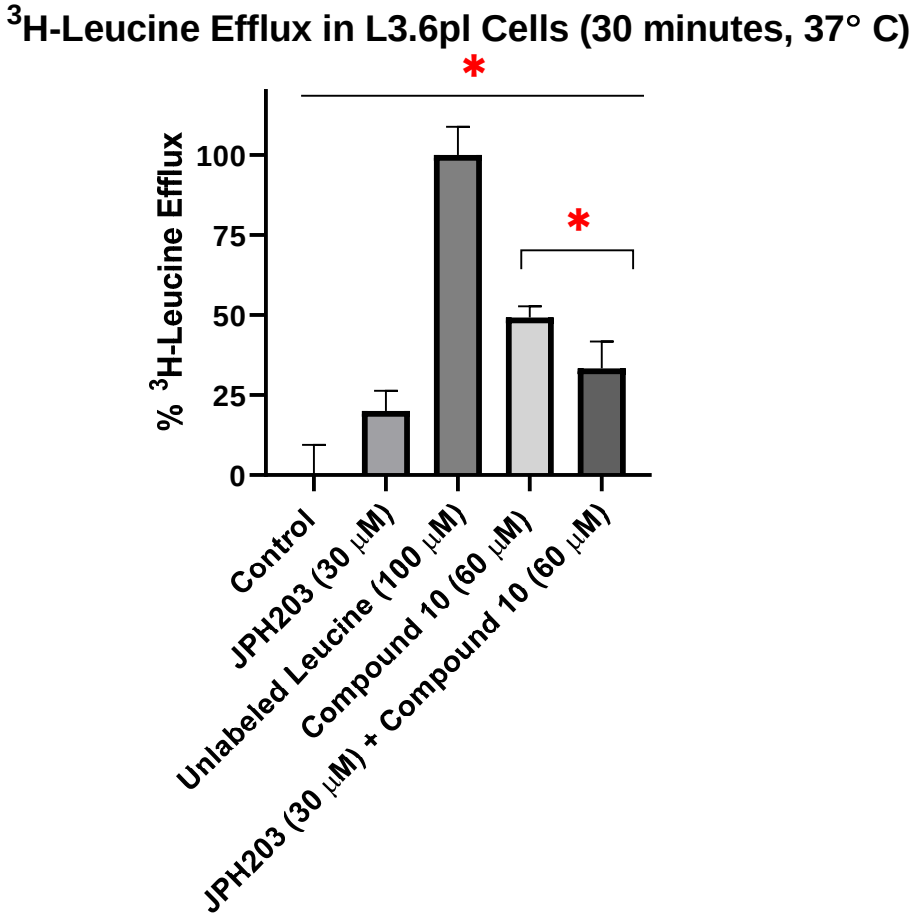

Figure 12. Leucine efflux agonism by compound **10** alone in L3.6pl cells after 30 min incubation at 37°C. The untreated control and unlabeled leucine experiments (Lanes 1 and 3) were performed as separate positive and negative controls, respectively, and were used here to define the range available for efflux agonism. JPH-203 was dosed at 30 μM (Lane 2) as a control to quantify any efflux stimulated by JPH-203 itself under these conditions. Compound **10** was dosed at 60 μM (Lane 4) and gave a statistically significant increase in ^{3}H-leucine efflux after 30 min incubation suggesting that it is, indeed, a leucine efflux agonist. The fact that the presence of the LAT-1 specific inhibitor JPH-203 significantly reduced the efflux induced by **10** (Lane 5) is consistent with LAT-1 targeting by compound **10**. Single asterisk indicates a p value <0.05.

The ability to starve cells of nutrients has gained significant attention in cancer research. For example, cis-platin-resistant growth of lung adenocarcinoma was found to be sensitive to periodic fasting and starvation-induced cell death, due to its dependence upon glutamine, which is required for nucleoside biosynthesis.[25] If a efflux agonist like **10** was cell selective and targeted LAT-1, then one would have the opportunity to selectively target and starve cancer cells with high expression of LAT-1. To assess whether **10** had any innate cell targeting specificity, we determined its 48h IC_{50} value in three cell lines. The 48 h IC_{50} values of compound **10** in L3.6pl, CHOK1, and CHO-MG cells were 3.48 ± 0.30 μM, 8.00 ± 0.56 μM, and 8.93 ± 0.75 μM, respectively. The IC_{50} values indicate that compound **10** is approximately two fold more toxic to L3.6pl cancer cells than to the CHO K1 and CHO-MG cell lines.

In Figure 8, we showed that compound **10** reduces the intracellular pools of spermidine and spermine in a dose-dependent manner. This finding was consistent with the ability of **10** to deplete intracellular methionine, which is normally used to biosynthesize these specific polyamines via decarboxylated SAM. In terms of targeting polyamine biosynthesis with **10**, we also investigated whether exogenous polyamines could rescue L3.6pl cells treated with **10**.

This was an important question to be answered because prior experience with the ODC inhibitor (i.e., DFMO) demonstrated that DFMO-treated L3.6pl cells could recover their growth by replenishing their depleted polyamine pools via spermidine import. [7] In addition, the AdoMetDC inhibitor (MDL73811) was shown to inhibit the growth of *P. falciparum* parasites and this growth inhibition was reversed by incubating infected erythrocytes with exogenous spermidine and spermine. This suggested that cells treated with this inhibitor could also be rescued by exogenous

polyamines.[26] In addition, prior work in L1210 murine leukemia cells demonstrated that inhibitors of AdoMetDC decrease intracellular spermidine and spermine levels, increase putrescine levels, and inhibit the growth of L1210 cells.[27] Addition of exogenous spermidine to L1210 cultures containing the AdoMetDC inhibitor was shown to restore normal growth rate.[27] These collective observations suggested that both ODC and AdoMetDC inhibition can be overcome via polyamine import.

Therefore, we ran a series of experiments to determine if cells treated with **10** could be rescued by exogenous polyamines. Briefly, L3.6pl cells were incubated for 72 h with an increasing dose of compound **10** and one of the native polyamines (putrescine, spermidine, or spermine; at a fixed dose of 1 μM or 5 μM). The results are shown in Figure 13.

We previously showed that L3.6pl cells were rescued to >90% of their growth in the presence of spermidine (1 μM) and an IC_{50} dose of DFMO.[7] Unlike the observations made with DFMO, none of the three native polyamines (at 1 μM or 5 μM) were able to rescue L3.6pl cells treated with compound **10** (at 5 μM or higher, Figure 13). Similarly, the native polyamines were also unable to rescue CHO-K1 and CHO-MG cells treated with a toxic concentration of compound **10** (results not shown). We also showed that compound **10** inhibits growth in a time-dependent manner, where longer incubation times (e.g., 72h) led to a greater reduction in cell growth compared to an untreated control (see Supporting Information).

These collective results suggested that the polyamine depletion induced by **10** cannot be overcome by polyamine import. This was a key finding because cancer cells often escape inhibitors of the polyamine biosynthetic enzymes (e.g., DFMO, AdoMetDC) via polyamine import.[7, 27] In short, facilitation of methionine export provides a novel way to deplete intracellular spermidine and

spermine pools without having to also inhibit polyamine import.[28] In this regard, compounds like **10** can be used to reduce intracellular polyamine pools in the presence of exogenous polyamines and obviate the need for a PTI. To support our planned future in vivo studies, we also determined that **10** was well tolerated over 24h, when injected i.p at 1 mg/kg in mice (n=2).

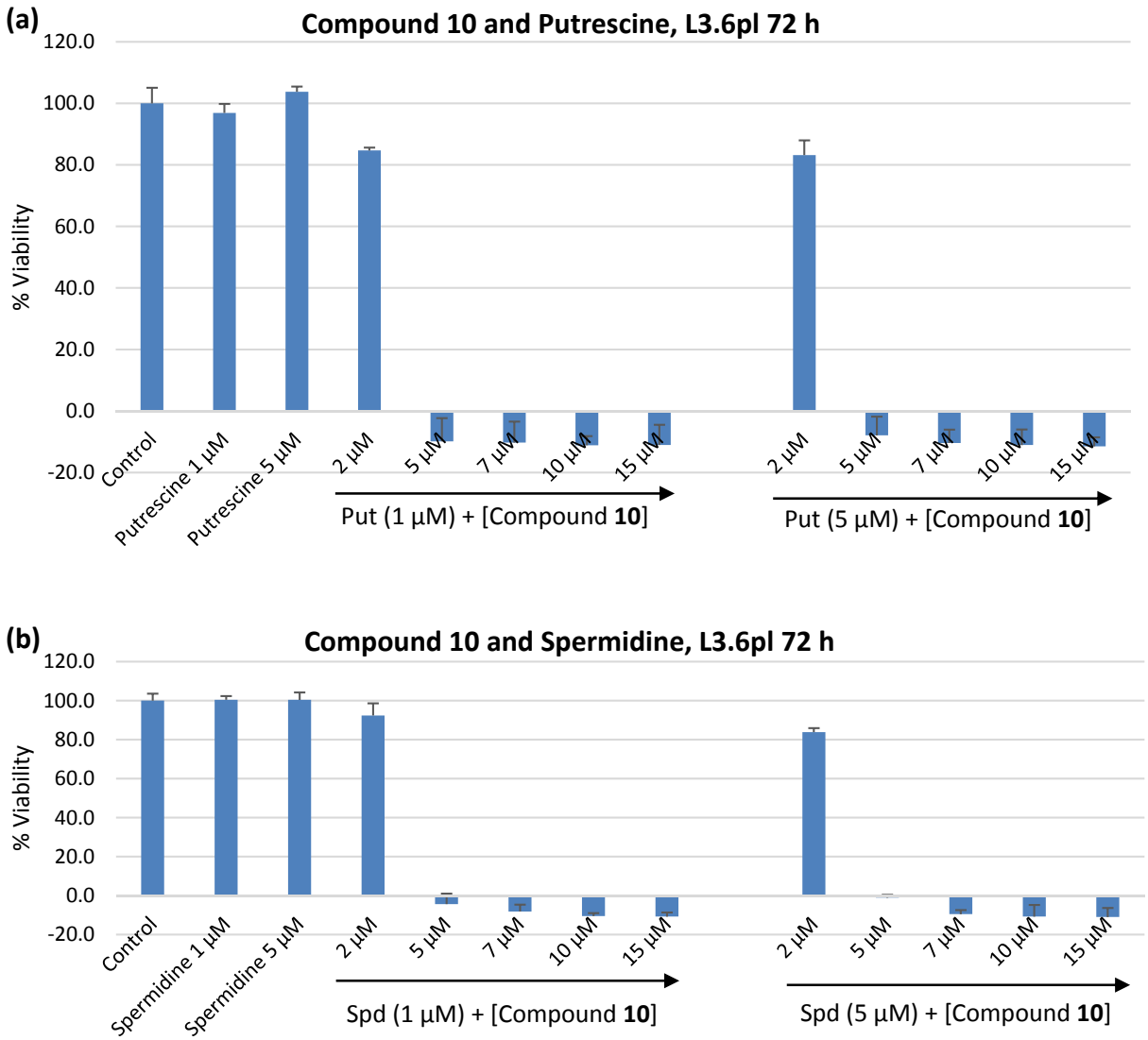

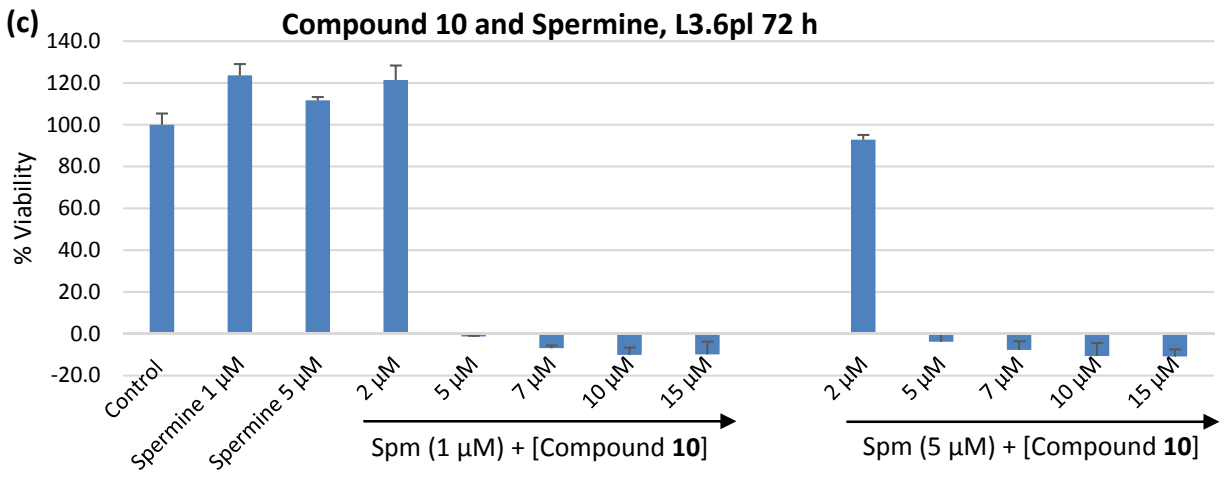

Figure 13. Inability of the native polyamines (a) putrescine (Put), (b) spermidine (Spd), and (c) spermine (Spm) at 1 µM and 5 µM to rescue L3.6pl cells treated with increasing concentrations of compound **10**. The L3.6pl cells were incubated with 250 µM aminoguanidine (AG) for 24 h prior to the addition of compound **10**, followed by 72 h incubation at 37°C. Columns 1-3 are control columns, with untreated L3.6pl pancreatic cancer cells as control and cells dosed with either 1 µM or 5 µM of the three native polyamines, respectively. Columns 4-8 and 9-13 show the results of experiments conducted with L3.6pl cells along with the respective native polyamine (fixed at either 1 or 5 µM) in the presence of increasing doses of **10**. None of the three native polyamines were able to rescue L3.6pl cells treated with toxic doses of **10**.

Conclusions. These studies suggest that compound **10** reduces intracellular levels of LAT-1 substrates, methionine and leucine, by inducing efflux of these amino acids. Our data suggests that compound **10** does not inhibit LAT-1 uptake like JPH-203, but instead may act as a LAT-1 efflux agonist. The profound reduction of intracellular methionine pools by **10** led to significant

reduction of intracellular spermidine and spermine pools in L3.6pl pancreatic cancer cells and inhibited cell growth.

As shown in Figure 1, limited methionine supply imparts several consequences for the cell including a likely reduction in the decarboxylated S-adenosylmethionine pools needed to provide the aminopropyl fragments required to biosynthesize the higher polyamines (Spd and Spm). In this regard, compounds like **10**, which affect methionine supply, can also disrupt polyamine homeostasis. Importantly, we showed that the availability of exogenous native polyamines (Put, Spd, or Spm) was unable to rescue cells treated with compound **10** (Figure 13). This finding is in direct contrast to the ODC inhibitor (DFMO), where polyamine import provides an escape pathway for cancer cells to circumvent the ODC inhibitor.[7]

As illustrated in Figure 1, we speculate that since SLC3A2 has been shown in independent reports to associate with either LAT-1 (in T24 human bladder carcinoma cells)[29] or SAT1,[30] it is possible that SLC3A2 provides a molecular bridge for the coupling of neutral amino acid import and polyamine acetylation/export. We note here, however, that we did not see a significant impact on the *N*-acetylspermidine or *N*-acetylspermine pools in the supernatants of cells in the presence or absence of the LAT inhibitor **10** (Table 1), which suggests that LAT-1/SLC3A2 and SAT1/SLC3A2 are likely independent transport systems. The ability to deplete intracellular polyamines as well as methionine and leucine pools with a single agent (e.g., **10**) provides a potent approach to control pancreatic cancer cell growth. Indeed, leucine itself is an important signaling molecule for the mTOR pathway, which is known to control PDAC cell fate[31] and proliferation in PC-2 pancreatic carcinoma cells.[32] Compound **10** now joins the growing list of LAT-targeting small molecules albeit with a novel mode of action (efflux agonism).[33-34] To the best of our knowledge, this is the first report of a LAT-1 efflux agonist. Future work will explore the role of

stereochemistry in these designs and evaluate the performance of **10** in models of pancreatic cancer.

EXPERIMENTAL

Materials. Silica gel 32-63 μm and chemical reagents were purchased from commercial sources and used without further purification. Unless otherwise noted, the ^{1}H NMR and ^{13}C NMR spectra were recorded at 500 MHz and 125 MHz, respectively. NH_4OH referred to concentrated aqueous ammonium hydroxide. All tested compounds provided satisfactory elemental analyses as proof of purity (≥ 95%) or were >95% pure by HPLC analysis. These are provided in the Supporting Information.

Biological Studies. CHO-K1 cells were obtained from ATCC, whereas CHO-MG cells were obtained from Dr. Wayne Flintoff at the University of Western Ontario. L3.6pl cells were obtained from Isaiah Fidler at the MD Anderson Cancer Center (Dallas, TX). CHO K1, CHO-MG, and L3.6pl cells were grown in RPMI 1640 medium supplemented with 10% fetal bovine serum (FBS) and 1% penicillin/streptomycin. All cells were grown at 37°C under a humidified 5% CO_2 atmosphere. Aminoguanidine (1 mM used for CHO K1 and CHOMG cells and 250 μM for L3.6pl) was added to the growth medium to prevent oxidation of the compounds of the bovine serum amine oxidase enzyme that is present in calf serum. The cells used were in early to mid-log phase and CHO and CHOMG were plated out at 1000 cells/well, whereas the L3.6pl cells were plated at 500 cells/well in a 96 well plate format.

Screening of Torrey Pines original library. A 96 well plate was received from TPIMS (Plate 110, shipped 2/5/2015) and each well contained 100 μL of a frozen 10% DMF/ water solution containing a complex mixture (1 mg/mL) of a molecular library based upon a specific molecular

scaffold. These samples were prepared at TPIMS by solid phase synthesis using the teabag approach. The original screen was run in triplicate using 10 μL of the solution from each well for each experiment. Briefly, a CHO-K1 cell suspension (170 μL, 1000 cells/well, containing 250 μM aminoguanidine) was plated out in 96 well format and incubated overnight at 37ºC to allow the cells time to adhere to the plate. Note: aminoguanidine was added to suppress the activity of the amine oxidase present in bovine serum, which would degrade the added spermidine. The following day, a phosphate buffered saline (PBS) solution of difluoromethylornithine (DFMO, 10 μL of 84 mM stock; final concentration of DFMO was 4.2 mM), spermidine (10 μL of 20 μM stock; 1 μM final concentration) and/or the molecular library sample (10 μL) or PBS (10 μL) was added to the respective wells so that the final volume was 200 μL. The plate was incubated for 48h at 37ºC in a 5% CO_2 atmosphere and relative growth assessed using the MTS reagent. Positive hits were compounds which gave a growth response similar to the DFMO-only control even though a rescuing dose of spermidine was present. These hits were then tested again for their ability to inhibit growth under the conditions of the assay. A positive hit had no growth inhibition when tested alone compared to an untreated control. This approach identified the library predicated upon the piperazine scaffold **A** (Figure 3) as a positive hit. This particular library, library **A**, contained ~31,320 compounds based upon the teabag approach used for its generation. To follow up on this discovery, additional plates were then received from TPIMS containing 192 members of the library **A** as 100 μM stock solutions of 'pure' compounds in 10% DMF/water. These were diluted with PBS and screened in the above assay. This follow-up screen using 'pure' compounds from TPIMS was conducted as described above with CHO-K1 cells using DFMO (4.2 mM, final concentration in well), spermidine (Spd, 1 μM), each TPIMS compound (5 μM) in 0.5% DMF and incubated for 48h at 37ºC in a 5% CO_2 atmosphere. Compounds **9** and **10** were found to be top

performers with no toxicity when tested alone and significant growth inhibition when tested with DFMO+Spd. Note: these hits were then resynthesized using our solution phase approach and retested to reconfirm these findings.

IC_{50} Determinations and Cell Viability Studies. Cell growth was assayed in sterile 96-well microtiter plates (Costar 3599, Corning, NY). CHO K1 or CHOMG cells were plated at 1,000 cells/70 μL and L3.6pl cells at 500 cells/70 μL. The drug solutions of appropriate concentration in phosphate buffered saline (PBS) were added 10 μL per well after overnight incubation. After drug exposure (e.g., for 48 h for CHO K1 and CHO-MG and 48h or 72 h for L3.6pl), cell growth was determined by measuring formazan formation from the 3-(4,5dimethylthiazol-2-yl)-5-(3-carboxymethoxyphenyl)-2-(4-sulfenyl)-2H-tetrazolium, inner salt (MTS) using SynergyMx Biotek microplate reader for absorbance (490 nm) measurements.[35] All experiments were run twice in triplicate.

72 h experiment with Compound 10 in L3.6pl cells. Each experiment was performed in triplicate. Ten milliliters of cell suspension containing L3.6pl human pancreatic cancer cells (50,000 cells/mL) and aminoguanidine (1 mM) was placed into separate poly-lysine treated plastic Petri dishes (d = 9 cm) and incubated overnight at 37˚ C. After 24 h, the cells were dosed with compound **10** at either 2 μM, 5 μM, or 7 μM. [Note: Stock solutions of **10** at 2, 5, and 7 mM were dissolved in phosphate buffered saline (PBS) and were filtered through a 0.2 μm filter prior to use]. The experiments were maintained with a total volume of 10.01 mL where 10 mL of the cell suspension was placed in a plastic dish and each compound or the equivalent PBS volume was added to make up the total volume 10.01 mL for each dish. For example, for the control experiment PBS (10 μL) was added to make up the total volume (10 mL + 10μL = 10.01 mL)]. After 72 h incubation at 37˚ C, the respective supernatants were collected first by pipetting off the supernatant

containing floating dead cells from the culture dish as well as media and placing them into 15 mL tubes. Each supernatant containing floating cells was centrifuged (4 min at 1,000 rpm). The cell-free supernatant (supernatant #1) was collected into a new 15 mL tube and quantified (~8.6 mL) and was then stored frozen and was later quantified by LCMS to investigate the media composition of particular polyamine and amino acid analytes. The attached cells remaining on the dish were washed with PBS (5 mL). The PBS wash was removed by suction and additional PBS (2 mL) was added and again suctioned off to provide twice-washed cells still adhered to the dish. Trypsin-EDTA (2 mL, 0.25% 1X, GIBCO) was then added to each dish and incubated (3-5 min at 37ºC) until all the cells were detached. Fresh media (8 mL) was added to quench the trypsin. The cell suspensions were then pipetted into separate 15 mL tubes and centrifuged (4 min at 1,000 rpm). The resulting supernatant was removed to provide a pellet. The pellet was suspended in PBS (10 mL) and was counted by a hemocytometer to provide cell counts for each experimental condition. The pellet was then centrifuged (4 min at 1,000 rpm) and the supernatant removed. The remaining cell pellet was quantified via protein and polyamine analysis.

To each cell pellet, a perchloric acid (150 μL) buffer solution (0.2M $HClO_4$/1M NaCl) and 0.9% NaCl (50 μL) was added. The samples were sonicated at room temperature via a Model 100 Fisher Scientific sonic dismembranator (in short 5 sec bursts at power level 7 setting) until samples were homogenized and cloudy. The homogenized samples were then vortexed and centrifuged (10 min at 4,000 rpm). The supernatants of the respective samples (supernatant #2) were removed and quantified by calibrated pipet (~190 μL volume). Note: 100 μL of supernatant #2 was placed into a micro-centrifuge tube for polyamine analysis by the *N*-dansylation HPLC protocol and the rest was placed into a different micro-centrifuge tube for analysis by LCMS of specific aminoacid analytes. The respective supernatants were stored in the freezer for polyamine and LCMS

quantification and the remaining protein pellet was used for the protein analysis. The protein pellet was dissolved in aq. NaOH (1 mM, 200 μL). The sample stood at room temperature with occasional vortex (45 min) and was then centrifuged (15 min at 15,000 rpm). The supernatant was collected and dissolved protein was quantified using the commercial Pierce BCA kit according to manufacturer's protocol using bovine serum albumin as a calibration standard.

Polyamine analysis protocol via *N*-dansylation and HPLC. Internal standard (1,7-diaminoheptane at 1.5×10^{-4}M) was added (30 μL) to supernatant #2 (100 μL sample) as well as 1M aqueous Na_2CO_3 solution (200 μL) and dansyl chloride (5 mg/mL) in acetone solution (400 μL). The sample mixture was vortexed and was then placed on a rotary shaker (65˚C for 60 min at 200 rpm). Proline solution (1M, 100 μL) was then added and the sample was placed on a rotary shaker (65˚C for 20 min at 200 rpm). The solution was transferred to a glass vial. Chloroform (1mL) was added and the vial was vigorously shook and placed on counter to allow the layers to separate and the top aqueous layer was removed by glass pipet. The sample was concentrated under reduced pressure using a rotary evaporator. Methanol was added (1 mL) to dissolve the remaining residue in the glass vial. Independent C_{18}-filter cartridges (Thermo Scientific hypersep C18, 50 mg bed weight) were 'pre-wetted' with methanol by eluting MeOH (1 mL) through with nitrogen gas. Then each dansylated polyamine methanol solution was added to the top of a pre-wetted cartridge and forced through with nitrogen gas and then additional methanol (0.5 mL) was added to the top and flushed through with nitrogen gas to collect the MeOH solution in a HPLC vial. Polyamine analysis was then performed via HPLC using gradient elution of acetonitrile and a heptanesulfonate aqueous buffer (pH 3.4) according to a published method. [36]

Protocol for Polyamine Level Determination in Figures 7 and 8. L3.6pl cells (500,000 cells/10 mL media) were incubated with aminoguanidine (250 μM) at 37°C for 24 h. Each compound was

then added either alone or in combination with other agents (e.g., Ant-44, 10 μL of appropriate stock solution) as indicated in Figures 7 and 8. The total volume in each dish was kept constant via the addition of PBS when needed, and the cells were incubated for another 72 h at 37°C. The cells were then washed extensively with ice cold PBS (once with 5 mL and twice with 2 mL). Each PBS wash was removed by suction. To the washed cells, an additional 2 mL of ice cold PBS was added and the cells were scraped off the dish and the suspension collected in a 5 mL centrifuge tube. The cell suspensions were then centrifuged at 1,000 rpm for 4 minutes to provide a cell pellet. The supernatant was carefully removed by suction. The cell pellet was lysed using a 0.2 M perchloric acid/1 M NaCl solution (200 μL), sonicated, and centrifuged. The resultant supernatant and pellet were separated. The supernatant volume was measured via calibrated pipet (~190 uL) and then used to quantify the respective *N*-dansylated polyamines by derivatization and HPLC analysis.[36] The protein content of the pellet was quantified using the Pierce BCA Protein assay kit from Thermo Scientific. Final results were expressed as nmol polyamine/mg protein. Each condition was performed in duplicate.

LCMS Analysis. The respective supernatant (10 μL) was injected on a Thermo HPLC system equipped with PAL CTC plate sampler (96-well plate), Dionex Ultimate 3000 binary pump (flow rate at 0.25 mL/ min), Dionex Ultimate 3000 thermostatted column compartment (temperature at 40°C), Thermo Endura Mass Spectrometer (ESI source), using Thermo Scientific Accucore C18 (2.6 μm, 2.1 x 50 mm, 100Å) column under a gradient of acetonitrile w/ 0.1% heptafluorobutyric acid (HFBA) in H_2O w/ 0.1% HFBA from 2% at minute 0 to 60% at minute 5.0, to 99% at minute 6.5 held until minute 7.5 and then reduced back to 2% until minute 10 to re-equilibrate the column for the next injection. The peak area was measured and analyte amounts were calculated referring to analyte calibration curves. Analyte levels were adjusted with internal standard concentration for

extraction efficiency. Peak height measurements were conducted referring to values obtained for standards of known concentrations. Calibration curves were constructed from eight concentrations (1, 5, 10, 50, 100, 500, 1000 and 5000 nM) by spiking 10 μL of 50x concentration DMSO stocks into 490 μL buffer and extracting 25 μL of the resulting sample and analyzing as detailed above. The LCMS data were originally reported in nM and then converted to pmoles analyte/mg protein by multiplying by the respective supernatant volume collected (e.g., supernatant #1, ~8.6 mL; supernatant #2, ~190 μL) and dividing by the mg of protein determined for the cell pellet by the BCA method obtained for that particular supernatant #1 and supernatant #2 sample. In this manner, the data for both the extracellular and intracellular analytes were expressed in the same pmol/mg protein units and are listed in the respective Tables.

Active vs. Passive Transport of L-Leucine, [4,5-^{3}H] control experiments. Cells were seeded individually in a 24 well plate (Costar 3524 Corning) at 60% confluency (100,000 cells/mL) in complete media and incubated overnight. The media was then replaced with Na^+ free Hanks' balanced salt solution (HBBS, 270 μL) containing 125 mM choline-Cl, 25 mM HEPES, 4.8 mM KCl, 1.2 mM $MgSO_4$, 1.2 mM KH_2PO_4, 1.3 mM $CaCl_2$ and 5.6 mM glucose (pH 7.4) and cells were further incubated for 10 minutes at 37° C. One plate was then pre-cooled to 4° C, while the other remained at 37° C. Each well with cells was then dosed with 30 μL of a 12 μM stock (for a final concentration of 1.2 μM) L-Leucine, [4,5-^{3}H] (79 Ci/mmol) (Moravek Biochemicals, Brea, California). Each plate was incubated at either 4° C or 37° C, after which cells were washed 3x with cold HBSS, lysed with 0.1% SDS mixed with 2 mL of scintillation fluid. Radioactivity was measured using a scintillation counter (Beckman Coulter LS 6500 Multi-Purpose Scintillation Counter). Transport was calculated by dividing counts per minute (CPM) of cells incubated at 4°

C by the counts obtained at 37°C. These experiments demonstrated the 40/60 ratio between outside bound leucine and internalized (imported) leucine.

Radiolabeled Leucine Uptake Assay. ^{3}H-Leucine uptake experiments were performed according to the protocol developed by Hafliger et al[24] with the following changes. Briefly, L3.6pl cells were seeded at 100,000 cells/1 mL in complete media (10% FBS, 1% penicillin/streptomycin in RPMI 1640), to produce 60% confluency in a 24-well plate and incubated for 4 h at 37°C. After 4 hours, the supernatant was removed and the cells were washed three times with 37°C pre-warmed Na+-free Hanks' balanced salt solution (HBSS, 240 µL) containing 125 mM choline-Cl, 25 mM HEPES, 4.8 mM KCl, 1.2 mM $MgSO_4$, 1.2 mM KH_2PO_4, 1.3 mM $CaCl_2$ and 5.6 mM glucose (pH 7.4) and further incubated in the same buffer at 37 °C for 10 min. Then, different concentrations of JPH-203 (10X stocks) in 30 µL were added. The cells were then dosed with 1.2 µM ^{3}H-L-leucine (30 µL of 12 µM stock of L-[^{3}H]leucine, 79 Ci/mmol). Uptake inhibition was measured for 15 minutes at 37ºC. Uptake was terminated by removing the buffer solution followed by washing the cells with cold Na+-free Hanks' Balanced Salt Solution (4ºC) three times. The remaining washed cells were then lysed with 0.1% SDS (500 µL) to give ~500 µL of cell lysate. A portion of the cell lysate (200 µL) was mixed with Scintiverse™ BD Cocktail (2 mL) for determining radiocounts. The radioactivity was measured with a scintillation counter (Beckman Coulter LS 6500 Multi-Purpose Scintillation Counter). The cpm vs JPH-203 graph is in Figure S3 and showed inhibition of ^{3}H-Leu uptake as expected for this LAT-1 inhibitor.

For compound **10**, a variety of conditions were examined (cases 1-3) and all of which failed to show inhibition of ^{3}H-leu uptake. In case 1, compound **10** simply replaced JPH-203 in the above protocol and showed no inhibition of ^{3}H-leucine uptake (data not shown). In an effort, to give compound **10** more time to reach its target, **10** was pre-incubated with L3.6pl cells for 24h, then

the cells were washed three times with 37°C pre-warmed Na+-free Hanks' balanced salt solution (HBSS, 240 µL) containing 125 mM choline-Cl, 25 mM HEPES, 4.8 mM KCl, 1.2 mM $MgSO_4$, 1.2 mM KH_2PO_4, 1.3 mM $CaCl_2$ and 5.6 mM glucose (pH 7.4) and further incubated in the same buffer at 37 °C for 10 min. At this point after 24h incubation, we envisioned two additional cases.

In case 2, compound **10** had reached its putative cellular target and remained bound after washing with buffer. Therefore, ^{3}H-leucine was added to the washed cells (with no compound **10** present) and incubated for 15 min at 37°C. Uptake was terminated by removing the buffer solution followed by washing the cells with cold Na+-free Hanks' Balanced Salt Solution (4°C) three times. The remaining washed cells were then lysed with 0.1% SDS (500 µL) to give ~500 µL of cell lysate. A portion of the cell lysate (200 µL) was mixed with Scintiverse™ BD Cocktail for determining radiocounts. The radioactivity was measured with a scintillation counter (Beckman Coulter LS 6500 Multi-Purpose Scintillation Counter). Another portion of the cell lysate (300 µL) was used for protein determination using the BCA method (Pierce). The final data was expressed as cpm/microgram of protein to account for the different number of cells remaining after the 24h experiment. This protocol also gave no inhibition of ^{3}H-Leu uptake as shown in Figure 9 (left).

In case 3 (after the 24h incubation, the media replacement step, and the HBSS incubation for 10 min step), compound **10** was back-added at the desired concentrations, followed by ^{3}H-leucine addition (within 4 min) and the cells incubated for 15 minutes at 37°C. Uptake was terminated by removing the buffer solution followed by washing the cells with cold Na+-free Hanks' Balanced Salt Solution (4°C) three times. The remaining washed cells were then lysed with 0.1% SDS (500 µL) to give ~500 µL of cell lysate. A portion of the cell lysate (200 µL) was mixed with Scintiverse™ BD Cocktail for determining radiocounts. The radioactivity was measured with a scintillation counter (Beckman Coulter LS 6500 Multi-Purpose Scintillation Counter). Another

portion of the cell lysate (300 μL) was used for protein determination using the BCA method (Pierce). The final data was expressed as cpm/microgram of protein to account for the different number of cells remaining after the 24h experiment and again did not show inhibition of ^{3}H-Leu uptake (Figure 9, right). In this regard, we made three separate efforts to observe inhibition of ^{3}H-Leu by compound **10** both at long (24h) and short times of incubation with **10** and L3.6pl cells. All of these assays with **10** failed to show inhibition of ^{3}H-Leu uptake.

Radiolabeled Leucine Efflux assay. ^{3}H-Leucine efflux experiments were performed according to the protocol developed by Hafliger et al. with the following changes.[24] Briefly, L3.6pl cells (100,000 cells in 270 μL) were preloaded with 30 μL of 12 μM stock of L-[^{3}H]leucine (79 Ci/mmol), to give a final concentration of 1.2 μM ^{3}H-leucine in each well. Cells were preloaded for 5 min at 37°C, then washed three times with cold Na^{+}-free HBSS. JPH-203 stock solutions were made in 3% DMSO and compound **10** and unlabeled leucine were each dissolved in PBS. For experiments with one additive (e.g., **10** alone) 270 μL of Na^{+}-free HBSS at rt was added followed by the addition of the single agent (e.g., compound **10** only) as a 10X stock solution (30 μL). For experiments with two additives (e.g., JPH-203 + unlabeled leucine), 240 μL of Na^{+}-free HBSS at rt was added followed by the addition of each agent (e.g., JPH-203 or unlabeled Leu) as a 10X stock solution (30 μL). The total volume in these assays was always 300 μL and either DMSO (30 μL) or PBS (30 μL) was added to the control wells so that the solvent composition was identical in all wells. The compounds and L3.6pl cells were incubated for either two minutes (Fig 9, Panel B and C) or thirty minutes (Fig 9, Panel D) at 37º C. The supernatant was then collected (300 μL) and mixed with scintillation fluid (Scintiverse™ BD Cocktail, 2 mL) and radioactivity measured (Beckman Coulter LS 6500 Multi-Purpose Scintillation Counter). The cells were then

washed three times with cold Na+-free HBSS (4ºC), then lysed to give ~300 µL of cell lysate. The lysate (300 µL) was mixed with scintillation fluid (2 mL) and radioactivity was counted. Relative efflux was expressed as percentage radioactivity = 100% x (radioactivity of medium)/(radioactivity of the medium + radioactivity of the cells). Data are shown in Figures 10-12 and the background obtained from the untreated control was subtracted as per the published Hafliger protocol.[24]

(S)-*N*-benzyl-2-((S)-3-benzyl-4-(3,3-dimethylbutyl)piperazin-1-yl)-3-phenylpropan-1-amine, trihydrochloride salt (9). Borane-tetrahydrofuran complex (1.0 M in THF, 1.98 mmol, 1.98 mL) was added via a syringe to **21** (130 mg, 0.247 mmol, 1 equiv) in distilled THF (3 mL) at ambient temperature. The mixture was then heated at 60-65 °C for 2 days. The reaction mixture was concentrated under reduced pressure to give a residue. A 10% concentrated HCl/Methanol solution (4 mL) was then added at 0^0C and stirred for 24 h. The mixture was then concentrated to give a residue. 1M NaOH was added until pH 10, and the solution was extracted three times with DCM, the organic layers were combined, dried over anhydrous Na_2SO_4, filtered, and concentrated. The crude triamine free base (107 mg) was purified by flash column chromatography (3% MeOH, 1% NH_4OH in DCM) to give the pure free base of **9** as a yellow oil (78 mg, 65%). A portion of the free base of **9** (45 mg) was dissolved in absolute ethanol (3 mL) at 0^0C. A 4 N HCl solution (6 mL) was slowly added to the free base solution. The solution was stirred for 30 minutes then concentrated. The resulting white solid was then taken up in water and concentrated to remove any remaining ethanol, giving the respective amine HCl salt of **9** (52 mg) as a crystalline solid. ^{1}H NMR (400 MHz, D_2O): δ 7.50-7.05 (m, 15H), 4.12 (m, 2H), 3.58-2.57 (m, 13H), 2.55-2.38 (m, 2H), 1.80-1.46 (m, 1H), 0.96 (s, 9H). ^{13}C NMR (100 MHz, D_2O): δ 139.3, 136.5, 131.9, 131.6,

131.5, 131.0, 130.8, 130.7, 130.6, 129.3, 128.6, 64.1, 63.2, 55.4, 52.9, 52.0, 51.8, 46.3, 42.9, 37.2, 35.8, 33.5, 30.8, 29.8. HPLC analysis (94.8% pure).

(R)-*N*-benzyl-3-cyclohexyl-2-((S)-3-isobutyl-4-isopentylpiperazin-1-yl)propan-1-amine, trihydrochloride salt (10). Borane-tetrahydrofuran complex (1.0 M, 3.9 mL, 3.9 mmol) was added via a syringe to **31** (236 mg, 0.488 mmol) in THF (6 mL) at ambient temperature. The mixture was then heated at 60-65 °C for 5 days. The reaction mixture was concentrated under reduced pressure to give a residue. A 10% concentrated HCl/methanol solution (8 mL) was then added at 0^0C and stirred for 24 h. The mixture was concentrated to give a residue. 1M NaOH was added until pH 10 and the solution then extracted three times with DCM. The organic layers were combined, dried over anhydrous Na_2SO_4, filtered, and concentrated. The crude triamine free base (176 mg) was purified by flash column chromatography (2% MeOH, 1% NH_4OH in DCM) to give the pure free base of **10** as a yellow oil (122 mg, 60%). Free base form of **10**: ^{1}H NMR (500 MHz, $CDCl_3$): δ 7.31 (m, 3H), 7.24 (m, 2H), 3.79 (m, 2H), 2.80-2.57 (m, 5H), 2.55-2.43 (m, 3H), 2.34 (m, 3H), 2.13 (m, 1H), 1.76-1.47 (m, 7H), 1.44-1.07 (m, 9H), 0.89 (m, 12H). ^{13}C NMR (500 MHz, $CDCl_3$): δ 140.5, 128.4, 126.8, 60.4, 58.1, 54.0, 51.7, 51.2, 49.7, 35.1, 34.32, 34.25, 33.1, 26.8, 26.6, 26.3, 26.2, 25.6, 24.1, 22.9, 22.7, 22.1. Anal. Calcd for $C_{29}H_{51}N_3 \cdot 0.4\ H_2O$, CHN.

Note: For long term storage the free base of **10** (106 mg) was dissolved in absolute ethanol (6 mL) at 0^0C. A 4 N HCl solution (12 mL) was slowly added to the free base solution. The solution was stirred for 30 minutes and then concentrated. The resulting white solid was then taken up in water and concentrated to remove any remaining ethanol, giving the respective amine HCl salt of **10** (131 mg) as a crystalline solid. HRMS *m/z* calc for $C_{29}H_{51}N_3$ $(M + H)^+$ theory: 441.4085, found: 441.4055.

(S)-methyl 2-(3,3-dimethylbutanamido)-3-phenylpropanoate (14). To a solution of 3,3-dimethylbutryic acid **12** (1.1 mL, 8.61 mmol, 1 equiv) and L-phenylalanine methyl ester hydrochloride **13** (1.86 g, 8.61 mmol, 1 equiv) in CH_2Cl_2 (40 mL) was added diisopropylethylamine (DIEA, 3.0 mL, 17.2 mmol, 2 equiv) followed by HATU (6.55 g, 17.2 mmol, 2 equiv) and stirred for 24 h at rt. The reddish brown reaction mixture turned milky white overnight. The reaction mixture was quenched by washing with aqueous saturated Na_2CO_3, followed by extraction with CH_2Cl_2. The organic layer was then separated, washed with water, dried over anhydrous Na_2SO_4, filtered and concentrated. The crude product was purified by column chromatography (100% $CHCl_3$) to give the pure coupled product **14** as a yellow oil (95%). ^{1}H NMR (500 MHz, $CDCl_3$): δ 7.31-7.22 (m, 3H), 7.11 (m, 2H), 5.76 (br s, 1H), 4.91 (m, 1H), 3.72 (s, 3H), 3.11 (m, 2H), 2.04 (s, 2H), 0.98 (s, 9H). ^{13}C NMR (500 MHz, $CDCl_3$): δ 172.2, 171.3, 135.9, 129.2, 128.6, 127.1, 52.9, 52.2, 50.3, 38.0, 30.9, 29.7. HRMS *m/z* calc for $C_{16}H_{23}NO_3$ $(M + H)^+$ theory: 277.1678, found: 277.1653. Anal. Chem. $C_{16}H_{23}NO_3$, CHN.

(S)-2-(3,3-dimethylbutanamido)-3-phenylpropanoic acid (15). 1M NaOH (7.6 mL, 7.6 mmol) was added slowly to methyl ester **14** (2.1 g, 7.57 mmol) in MeOH (75 mL) at 0ºC with stirring. The mixture was allowed to warm to room temperature and stir until consumption of the methyl ester was observed by TLC (1% MeOH in DCM). After 24 hours, the reaction mixture was concentrated under reduced pressure. The resulting oil was then cooled to 0ºC and a white precipitate formed upon addition of 0.1 M HCl (130 mL). Vacuum filtration was used to collect the solid. Note: the filtrate was extracted two times with ethyl acetate and the organic layer was dried over anhydrous Na_2SO_4, filtered, and concentrated to increase yield of the solid **15** (1.98 g, 99 %). ^{1}H NMR ($CDCl_3$) confirmed the loss of the methyl ester singlet of **14** (3.73 ppm) and the generated carboxylic acid **15** was consumed in the next step. ^{1}H NMR (500 MHz, $CDCl_3$): δ 7.33-

7.24 (m, 3H), 7.19 (m, 2H), 5.74 (m, 1H), 4.84 (td, 1H, $J^3_{H\text{-}H}$ = 7.2 Hz, 7.2 Hz, 5.6 Hz), 3.19 (m, 2H), 2.05 (m, 2H), 0.94 (s, 9H). HRMS *m/z* calc for $C_{15}H_{21}NO_3$ $(M + H)^+$ theory: 263.1521, found: 263.1547. Anal. Chem. $C_{15}H_{21}NO_3$, CHN.

***N*-((S)-1-(((S)-1-amino-1-oxo-3-phenylpropan-2-yl)amino)-1-oxo-3-phenylpropan-2-yl)-3,3-dimethylbutanamide (17).** To the solution of 2-(3,3-Dimethyl-butyrylamino)-3-phenyl-propionic acid **15** (773 mg, 2.93 mmol) and L-phenylalanine amide **16** (488 mg, 2.97 mmol) in DCM (25 mL) was added DIEA (1.02 mL, 5.87 mmol), followed by HATU (2.34 g, 6.15 mmol) and stirred for 3 days at room temperature. A white precipitate formed over the course of the reaction. The reaction was filtered and the resulting precipitate was taken up in hot ethyl acetate and washed with 0.1 M HCl, aqueous Na_2CO_3, and water. The organic layer was dried over anhydrous Na_2SO_4, filtered, and concentrated to yield the pure triamide **17** as a white solid (464 mg, 39%). ^{1}H NMR (500 MHz, d_6-DMSO): δ 7.90 (m, 2H), 7.34-7.05 (m, 12H), 4.51 (m, 1H), 4.43 (m, 1H), 2.98 (m, 2H), 2.84 (m, 1H), 2.68 (m, 1H), 1.89 (s, 2H), 0.77 (s, 9H). ^{13}C NMR (500 MHz, d_6-DMSO): δ 172.6, 171.2, 170.8, 138.0, 137.7, 129.2, 129.1, 128.0, 127.9, 126.2, 126.1, 53.8, 53.6, 48.5, 37.6, 37.2, 30.3, 29.5. HRMS *m/z* calc for $C_{24}H_{31}N_3O_3$ $(M + H)^+$ theory: 409.2365, found: 409.2386. Anal. Chem. $C_{24}H_{31}N_3O_3$, CHN.

(S)-N^1-((S)-1-amino-3-phenylpropan-2-yl)-N2-(3,3-dimethylbutyl)-3-phenylpropane-1,2-diamine (18). Borane-tetrahydrofuran complex (1.0 M in THF, 13.7 mmol, 8 equiv., 13.7 mL) was added via a syringe to *N*-[1-(1-Carbamoyl-2-phenyl-ethylcarbamoyl)-2-phenyl-ethyl]-3,3-dimethyl-butyramide **17** (700 mg, 1.71 mmol, 1 equiv) in THF (43 mL) at ambient temperature. The mixture was then heated at 60-65 °C. After refluxing for 4 days, the reaction mixture was concentrated under reduced pressure to give a residue. A 10% concentrated HCl/MeOH solution (30 mL) was then added at 0^{0}C and stirred for 24 h. The mixture was concentrated to give a

residue, which was taken up in 1M NaOH until reaching pH 10, then extracted three times with DCM, the organic layers were combined, dried over anhydrous Na_2SO_4, filtered, and concentrated. The crude triamine free base (610 mg) was purified by flash column chromatography (5% MeOH, 1% NH_4OH in DCM) to give the pure triamine **18** as a yellow oil (330 mg, 52%). ^{1}H NMR (500 MHz, $CDCl_3$): δ 7.20 (m, 4H), 7.13 (m, 2H), 7.05 (m, 4H), 2.74 (m, 2H), 2.70-2.34 (m, 10H), 1.23 (m, 2H), 0.79 (s, 9H). ^{13}C NMR (500 MHz, $CDCl_3$): δ 139.12, 139.06, 129.01, 128.98, 128.14, 128.12, 125.9, 125.8, 61.3, 59.4, 53.3, 49.3, 44.3, 43.9, 42.9, 38.8, 29.3.

***N*-((S)-2-(((S)-2-((3,3-dimethylbutyl)amino)-3-phenylpropyl)amino)-3-phenylpropyl)-benzamide (20).** A solution of *N*-(benzoyloxy)succinimide **19** (213 mg, 0.97 mmol) in DCM (2 mL) was added dropwise to a stirred solution of triamine **18** (358 mg, 0.97 mmol) in DCM (2 mL) at 0^{o}C. The reaction mixture was allowed to warm to room temperature and stirred until TLC (7% MeOH, 1% NH_4OH in DCM) showed complete consumption of the starting material. After 19 h, the reaction mixture was washed with aqueous saturated Na_2CO_3, dried over anhydrous Na_2SO_4, filtered, and concentrated to give a crude residue. The crude residue was purified by flash column chromatography (3% MeOH, 1% NH_4OH in DCM) to give pure diamine **20** as an oil (412 mg, 90%). ^{1}H NMR (500 MHz, $CDCl_3$): δ 7.73 (m, 2H), 7.41 (m, 1H), 7.34 (m, 2H), 7.26-7.07 (m, 12H), 7.00 (m, 2H), 3.47 (dt, 1H, $J^2_{H\text{-}H}$ = 13.6 Hz, $J^3_{H\text{-}H}$ = 4.6 Hz, 4.6 Hz), 3.32 (dt, 1H, $J^2_{H\text{-}H}$ = 13.6 Hz, $J^3_{H\text{-}H}$ = 6.0 Hz, 6.0 Hz), 2.97 (m, 1H), 2.81-2.35 (m, 10H), 1.11 (m, 2H). ^{13}C NMR (500 MHz, $CDCl_3$): δ 167.6, 138.6, 138.3, 134.7, 131.3, 129.2, 129.1, 128.7, 128.54, 128.45, 127.1, 127.0, 126.9, 126.6, 126.4, 59.4, 58.5, 48.4, 43.7, 42.9, 42.4, 39.4, 38.6, 29.7, 29.6, 29.52, 29.45. HRMS *m/z* calc for $C_{31}H_{41}N_3O$ $(M + H)^+$ theory: 471.3250, found: 471.3211. Anal. Chem. $C_{31}H_{41}N_3O$, CHN.

***N*-((S)-2-((S)-5-benzyl-4-(3,3-dimethylbutyl)-2,3-dioxopiperazin-1-yl)-3-phenylpropyl)-benzamide (21).** To a solution of diamine **20** (0.02 M, 197 mg, 0.42 mmol) in DCM (10 mL) at 0^0C was slowly added a 5-fold excess of oxalyldiimidazole (0.1 M, 397 mg, 2.1 mmol) in DCM (11 mL). The resulting reaction mixture was allowed to stir at room temperature for 3h and monitored by TLC (7% MeOH, 1% NH_4OH in DCM). The reaction mixture was deemed complete by TLC and was concentrated under reduced pressure. The crude reaction residue (603 mg) was purified by column chromatography (40% EtOAc, 1.5% EtOH in hexanes) to give the pure cyclized product **21** as a white powder (173 mg, 79%). ^{1}H NMR (500 MHz, $CDCl_3$): δ 7.78 (d, 1H, $J^3_{H\text{-}H}$ = 7.3 Hz), 7.40 (m, 1H), 7.32 (m, 2H), 7.24-7.10 (m, 9H), 6.80 (d, 2H, $J^3_{H\text{-}H}$ = 7.3 Hz), 4.58 (br s, 1H), 3.92 (m, 1H), 3.58 (m, 3H), 3.37 (m, 1H), 3.16 (m, 1H), 3.06 (d, 1H, $J^2_{H\text{-}H}$ = 13.2 Hz), 2.94 (d, 1H, $J^3_{H\text{-}H}$ = 6.6 Hz) 2.56 (m, 1H), 2.44 (m, 2H), 1.29 (td, 1H, $J^2_{H\text{-}H}$ = 12.3 Hz, 12.3 Hz), 1.18 (m, 2H), 0.73 (s, 9H). ^{13}C NMR (500 MHz, $CDCl_3$): δ 208.8, 205.4, 166.9, 158.0, 155.6, 140.7, 135.6, 132.7, 130.5, 127.98, 127.95, 127.90, 127.87, 127.5, 126.19, 126.16, 126.1, 55.3, 42.5, 41.0, 39.8, 36.8, 35.0, 28.7, 28.1. HRMS *m/z* calc for $C_{33}H_{39}N_3O_3$ $(M + H)^+$ theory: 525.2991, found: 525.2991. Anal. Chem. $C_{33}H_{39}N_3O_3$, CHN.

(S)-ethyl 4-methyl-2-(3-methylbutanamido)pentanoate (24). A procedure similar to that described above for **14** was used to prepare **24** using isovaleric acid **22** and L-leucine ethyl ester hydrochloride **23**. After 24 h, the TLC (2% MeOH in DCM) showed disappearance of the starting material. The reaction mixture was quenched by washing with aqueous Na_2CO_3, followed by extraction with DCM. The organic layer was collected and washed with 0.01 M HCl. The resulting organic layer was collected and washed with water, then dried over anhydrous Na_2SO_4, filtered, and concentrated. The crude was purified by flash column chromatography using 0.5% MeOH in DCM to give the pure coupled product **24** as a white solid (93%). ^{1}H NMR (500 MHz, $CDCl_3$): δ

5.93 (d, 1H, $J^3_{H\text{-}H}$ = 8.1 Hz), 4.64 (td, 1H, $J^3_{H\text{-}H}$ = 8.7 Hz x 2), 4.18 (q, 2H, $J^3_{H\text{-}H}$ = 7.3 Hz x 3), 2.17-2.06 (m, 3H), 1.66 (m, 2H), 1.54 (m, 1H), 1.28 (t, 3H, $J^3_{H\text{-}H}$ = 7.2 Hz x 2), 0.95 (m, 11H). ^{13}C NMR (500 MHz, $CDCl_3$): δ 173.2, 172.2, 61.2, 50.5, 45.9, 41.7, 26.1, 24.8, 22.8, 22.4, 21.9, 14.1. HRMS *m/z* calc for $C_{13}H_{25}NO_3$ $(M + H)^+$ theory: 244.1907, found: 244.1909. Anal. Chem. $C_{13}H_{25}NO_3$, CHN.

(S)-4-methyl-2-(3-methylbutanamido)pentanoic acid (25). Aqueous NaOH (1M, 3 mL, 3 mmol) was added slowly to ethyl ester **24** (710 mg, 2.92 mmol) in MeOH (29 mL) at 0°C with stirring. The mixture was allowed to warm to room temperature. Consumption of the starting ethyl ester was observed by TLC (2% MeOH in DCM) after 5 h. The reaction mixture was concentrated under reduced pressure. The resulting oil was then cooled to 0°C and 50 mL of 0.1 M HCl added. The pH of the aqueous phase was checked to ensure it was acidic (pH 2). The aqueous phase was extracted three times with DCM (see note below*), and the organic layers were combined, dried over anhydrous Na_2SO_4, filtered and concentrated to give the carboxylic acid **25** as a white powder (88%) with no further purification. *Note: later experiments revealed that ethyl acetate was a more efficient extraction solvent than DCM for this step. ^{1}H NMR ($CDCl_3$) confirmed the loss of the ethyl ester. ^{1}H NMR (500 MHz, $CDCl_3$): δ 5.77 (d, 1H, $J^3_{H\text{-}H}$ = 7.1 Hz), 4.60 (ddd, 1H, $J^3_{H\text{-}H}$ = 9.2 Hz, 7.8 Hz, 5.0 Hz), 2.12 (m, 3H) 1.78-1.67 (m, 2H), 1.59 (m, 1H), 0.96 (m, 12H).

(R)-methyl 3-cyclohexyl-2-((S)-4-methyl-2-(3-methylbutanamido)pentanamido)propanoate (27). To a solution of **25** (423 mg, 1.96 mmol) and D-cyclohexylalanine methyl ester hydrochloride **26** (436 mg, 1.96 mmol) in DCM (15 mL) was added DIEA (0.92 mL, 5.3 mmol, 2.7 equiv) followed by HATU (1.49 g, 3.92 mmol, 2 equiv). The resulting mixture was stirred overnight at rt. After 22 h, TLC (5% MeOH in DCM) showed disappearance of the starting

materials. The reaction mixture was worked up by washing with saturated aqueous Na_2CO_3, followed by extraction with DCM. The organic layer was separated and washed with 0.01 M HCl. The organic layer was again separated and the remaining aqueous layer was extracted with additional DCM. The resulting organic layers were combined and washed once with water, dried over anhydrous Na_2SO_4, filtered and concentrated. The crude orange solid (1.04 g) was purified through flash column chromatography (1% MeOH in DCM) to give the pure coupled product **27** as a white solid (717 mg; 96%). ^{1}H NMR (500 MHz, $CDCl_3$): δ 6.57 (d, 1H, $J^3_{H\text{-}H}$ = 8.1 Hz), 5.82 (d, 1H, $J^3_{H\text{-}H}$ = 6.8 Hz), 4.49 (m, 2H), 3.63 (s, 3H), 2.03 (m, 3H), 1.80-1.52 (m, 9H), 1.46 (m, 2H), 1.29-0.99 (m, 5H), 0.88 (m, 12H). ^{13}C NMR (500 MHz, $CDCl_3$): δ 173.1, 172.7, 171.8, 52.2, 51.3, 50.2, 45.9, 40.8, 39.8, 34.2, 33.5, 32.4, 26.3, 26.2, 26.0, 24.9, 22.8, 22.42, 22.37, 22.2. HRMS *m/z* calc for $C_{21}H_{38}N_2O_4$ $(M + H)^+$ theory: 382.2832, found: 382.2820. Anal. Chem. $C_{21}H_{38}N_2O_4$, CHN.

(S)-*N*-((R)-1-amino-3-cyclohexyl-1-oxopropan-2-yl)-4-methyl-2-(3-methylbutanamido)-pentanamide (28). To a solution of **27** (680 mg, 1.78 mmol) in MeOH (20 mL) was added a vigorous stream of NH_3 gas at 0^0C with stirring. After 1 hr, the introduction of ammonia gas is discontinued and the flask closed with a glass stopper. The reaction solution was allowed to warm to room temperature and stirred for five days. After the first two days, a stream NH_3 gas was reintroduced for an additional hour. The solvent was removed under reduced pressure after 5 days to give the crude triamide product as a cream colored solid (670 mg). The crude solid was taken up in cold DCM (50 mL) and filtered to give the pure triamide **28** as a white solid (534 mg, 82%). ^{1}H NMR (500 MHz, d_6-DMSO): δ 8.26 (d, 1H, $J^3_{H\text{-}H}$ = 8.3 Hz), 8.02 (d, 1H, $J^3_{H\text{-}H}$ = 6.6 Hz), 7.27 (s, 1H), 7.01 (s, 1H), 4.18 (m, 2H), 1.97 (m, 3H), 1.68-1.34 (m, 11H), 1.17-1.00 (m, 2H), 0.91 (m, 4H), 0.85 (m, 11H). HRMS *m/z* calc for $C_{20}H_{37}N_3O_3$ $(M + H)^+$ theory: 367.2835, found: 367.2871. Anal. Chem. $C_{20}H_{37}N_3O_3$, CHN.

(S)-*N*^{1}-((R)-1-amino-3-cyclohexylpropan-2-yl)-N2-isopentyl-4-methylpentane-1,2-diamine (29). Borane-tetrahydrofuran complex (1.0 M in THF, 11 mmol, 11 mL) was added via a syringe to triamide **28** (505 mg, 1.37 mmol) in THF (15 mL) at ambient temperature. The reaction mixture was heated at 60-65 °C for 2 days and was then concentrated under reduced pressure to give a residue. A 10% concentrated HCl/methanol solution was then added at 0^0C and stirred for 24 h. The mixture was concentrated to give a white residue. 1M NaOH was added until pH 10, and the solution was then extracted three times with DCM. The respective organic layers were combined, dried over anhydrous Na_2SO_4, filtered, and concentrated to give triamine free base **29** as an oil (97%) without further purification. ^{1}H NMR (500 MHz, $CDCl_3$): δ 2.71-2.39 (m, 7H), 2.31 (dd, 1H, $J^2_{H\text{-}H}$ = 11.7 Hz, $J^3_{H\text{-}H}$ = 6.8 Hz), 1.60 (m, 6H), 1.33-1.02 (m, 11H), 0.83 (dd, 1H, $J^3_{H\text{-}H}$ = 6.6 Hz, $J^3_{H\text{-}H}$ = 3.2 Hz). ^{13}C NMR (500 MHz, $CDCl_3$): δ 56.9, 56.0, 50.2, 45.4, 45.0, 42.6, 40.7, 39.6, 34.6, 33.9, 33.7, 26.6, 26.4, 26.2, 25.1, 23.2, 22.9, 22.73, 22.70.

***N*-((R)-3-cyclohexyl-2-(((S)-2-(isopentylamino)-4-methylpentyl)amino)propyl)benzamide (30).** A solution of *N*-(benzoyloxy)succinimide (259 mg, 1.18 mmol, 0.89 equiv) in DCM (2 mL) was added dropwise to a stirred solution of triamine **29** (434 mg, 1.33 mmol) in DCM (2 mL) at 0^0C. The reaction mixture was allowed to warm to room temperature and stirred for 20 h. After TLC (7% MeOH, 1% NH_4OH in DCM) showed complete consumption of the starting material (20 h), the reaction mixture was washed with saturated aqueous Na_2CO_3, dried over anhydrous Na_2SO_4, filtered, and concentrated to give a crude residue. The crude was purified by column chromatography (2% MeOH, 1% NH_4OH in DCM) to give pure **30** as an oil (73%). ^{1}H NMR (500 MHz, $CDCl_3$): δ 7.81 (m, 2H), 7.47 (m, 1H), 7.41 (m, 2H), 7.18 (br s, 1H), 3.57 (dt, 1H, $J^2_{H\text{-}H}$ = 13.6 Hz, $J^3_{H\text{-}H}$ = 4.4 Hz, 4.4 Hz), 3.27 (dt, 1H, $J^2_{H\text{-}H}$ = 13.4 Hz, $J^3_{H\text{-}H}$ = 5.6 Hz, 5.6 Hz), 2.84 (m, 1H), 2.79 (dd, 1H, $J^2_{H\text{-}H}$ = 11.7 Hz, $J^3_{H\text{-}H}$ = 3.7 Hz), 2.66 (m, 1H), 2.58 (m, 2H), 2.44 (dd, 1H, $J^2_{H\text{-}}$

$_H$ = 11.7 Hz, $J^3_{H\text{-}H}$ = 6.1 Hz), 1.70 (m, 4H), 1.60 (m, 2H), 1.44-1.10 (m, 11H), 0.88 (m, 14H). ^{13}C NMR (500 MHz, $CDCl_3$): δ 167.4, 134.8, 131.2, 128.4, 127.0, 55.8, 54.0, 48.9, 45.3, 42.33, 42.26, 41.0, 39.4, 34.4, 33.6, 26.5, 26.3, 26.2, 25.1, 23.1, 22.70, 22.66, 22.6. HRMS *m/z* calc for $C_{27}H_{47}N_3O$ $(M + H)^+$ theory: 429.3719, found: 429.3719. Anal. Chem. $C_{27}H_{47}N_3O \cdot 0.2H_2O$, CHN.

***N*-((R)-3-cyclohexyl-2-((S)-5-isobutyl-4-isopentyl-2,3-dioxopiperazin-1-yl)propyl)-benzamide (31).** To a solution of diamine **30** (330 mg, 0.77 mmol) in DCM (18 mL) at 0^{0}C was slowly added a 5-fold excess of oxalyldiimidazole (0.1 M, 730 mg, 3.84 mmol) in DCM (20 mL). The resulting reaction mixture was allowed to stir at rt for 3 days until complete consumption of the starting material was observed by TLC (7% MeOH, 1% NH_4OH in DCM). The mixture was then concentrated under reduced pressure. The crude residue (1 g) was purified by flash column chromatography (2% MeOH in DCM) to give the pure cyclized product **31** as a white powder (307 mg, 82%). ^{1}H NMR (500 MHz, $CDCl_3$): δ 7.75 (m, 2H), 7.45 (m, 1H), 7.38 (m, 2H), 7.00 (br s, 1H), 4.83 (m, 1H), 3.91 (m, 2H), 3.67 (dd, 1H, $J^2_{H\text{-}H}$ = 13.0 Hz, $J^3_{H\text{-}H}$ = 4.2 Hz), 3.40 (m 1H), 3.28 (dt, 1H, $J^2_{H\text{-}H}$ = 14.1 Hz, $J^3_{H\text{-}H}$ = 3.9 Hz, 3.9 Hz), 3.23 (dd, 1H, $J^2_{H\text{-}H}$ = 13.2 Hz), 2.80 (m, 1H), 1.93 (d, 1H, $J^2_{H\text{-}H}$ = 12.7 Hz), 1.69 (m, 5H), 1.59-1.31 (m, 7H), 1.30-1.09 (m, 4H), 0.92 (dd, 6H, $J^3_{H\text{-}H}$ = 8.6 Hz, $J^3_{H\text{-}H}$ = 6.6 Hz), 0.84 (dd, 6H, $J^3_{H\text{-}H}$ = 8.6 Hz, $J^3_{H\text{-}H}$ = 6.6 Hz). ^{13}C NMR (500 MHz, $CDCl_3$): δ 168.0, 158.7, 156.3, 133.9, 131.5, 128.6, 127.1, 51.8, 44.3, 41.6, 40.1, 37.1, 36.6, 34.4, 34.0, 32.7, 26.4, 26.2, 26.1, 25.9, 25.2, 23.3, 22.6, 22.2, 21.2. HRMS *m/z* calc for $C_{29}H_{45}N_3O_3$ $(M + H)^+$ theory: 483.3461, found: 483.3451. Anal. Chem. $C_{29}H_{45}N_3O_3$, CHN.

Supporting Information. ^{1}H and ^{13}C NMR spectra of compounds **9, 10, 14, 17, 18, 20, 21, 24,** and **27-31** as well as ^{1}H NMR spectra for synthetic intermediates **15** and **25**, elemental analyses for compounds **10**, **14, 15, 17, 20, 21, 27, 28, 30**, and **31**, HPLC purity check for **9,** images of cells treated with Ant44 and **10**, time course study showing reduced growth of L3.6pl cells in the

presence of compound **10** over 24, 48, and 72h periods, cytotoxicity curves for compounds **9** and **10** in CHO-K1 cells and inhibition of ^{3}H-leucine uptake by JPH-203 in L3.6pl cells. A CSV file is also available which summarizes the bioactivities observed. These are available online at www.pubs.acs.org.

Corresponding Author Information: Dr. Otto Phanstiel, 12722 Research Parkway, Orlando, FL 32826; otto.phanstiel@ucf.edu ; 407-823-6545, fax 407-384-2062

Author Contributions. CM, OP, and HM developed and conducted the organic syntheses and CM, JT, HI, and SD conducted the bioevaluation experiments. CM and OP wrote the manuscript.

Acknowledgments. The authors wish to thank the UCF College of Medicine for their financial support of this work (grant #25014202) and Dr. Adel Nefzi at the TPIMS for access to the TPIMS molecular libraries as part of the Florida Drug Discovery Acceleration Program.

Abbreviations:

acetyl-CoA	acetyl-coenzyme A
AdoDATO	*S*-adenosyl-1,8-diamino-3-thio-octane
AdoMetDC	*S*-adenosylmethionine decarboxylase
AG	aminoguanidine
Ant-44	N^1-(9-anthracenylmethyl)-homospermidine
APAO	Acetylpolyamine oxidase
CDAP	*N*-(3-aminopropyl)-cyclohexylamine
CHO K1	Chinese hamster ovary cells K1
CHO-MG	Chinese hamster ovary cells deficient in polyamine transport
DCM	dichloromethane
DFMO	α-Difluoromethylornithine
DIEA	diethylisopropylamine
DMSO	dimethylsulfoxide
FBS	fetal bovine serum
HATU	(1-[Bis(dimethylamino)methylene]-1*H*-1,2,3-triazolo[4,5-*b*]pyridinium-3-oxide hexafluoro-phosphate
HFBA	heptafluorobutyric acid
HPLC	high performance liquid chromatograph
HRMS	high resolution mass spectrometry
LAT	large neutral aminoacid transporter
LAT-1	large neutral aminoacid transporter 1
LC-MS	liquid chromatograph-mass spectrometer
MAT	methionine adenosyltransferase
MCHA	*trans*-4-methylcyclohexylamine
MeOH	methanol
MTC	maximum tolerated concentration

mTOR	mechanistic/mammalian target of rapamycin
MTS	3-(4,5dimethylthiazol-2-yl)-5-(3-carboxymethoxyphenyl)-2-(4-sulfenyl)-2H-tetrazolium, inner salt
ODC	ornithine decarboxylase
PBS	phosphate buffered saline
PTI	Polyamine transport inhibitor
PTS	polyamine transport system
Put	putrescine
p70S6K	p70 ribosomal S6 kinase 1
SAM	*S*-adenosyl-L-methionine
SAT-1	spermine/spermidine N^1-acetyltransferase
SLC7A5	solute carrier 7A5, LAT-1
SLC3A2	solute carrier 3A2
SMOX	spermine oxidase
SMS	spermine synthase
Spd	spermidine
Spm	spermine
SRM	spermidine synthase
THF	tetrahydrofuran
TPIMS	Torrey Pines Institute for Molecular Studies
4E-BP1	initiation factor 4E binding protein
4F2HC	SLC3A2 alias

References

1. Casero, R. A., Jr.; Marton, L. J., Targeting polyamine metabolism and function in cancer and other hyperproliferative diseases. *Nature Rev Drug Discov* **2007,** *6* (5), 373-390.

2. Igarashi, K.; Kashiwagi, K., Modulation of cellular function by polyamines. *Int J Biochem Cell Biol* **2010,** *42* (1), 39-51.

3. Russell, D.; Snyder, S. H., Amine synthesis in rapidly growing tissues: ornithine decarboxylase activity in regenerating rat liver, chick embryo, and various tumors. *Proc Natl Acad Sci U S A* **1968,** *60* (4), 1420-1427.

4. Russell, D. H., The roles of the polyamines, putrescine, spermidine, and spermine in normal and malignant tissues. *Life Sci* **1973,** *13* (12), 1635-1647.

5. Mandal, S.; Mandal, A.; Johansson, H. E.; Orjalo, A. V.; Park, M. H., Depletion of cellular polyamines, spermidine and spermine, causes a total arrest in translation and growth in mammalian cells. *Proc Natl Acad Sci U S A* **2013,** *110* (6), 2169-2174.

6. Kahana, C., Regulation of cellular polyamine levels and cellular proliferation by antizyme and antizyme inhibitor. *Essays Biochem* **2009,** *46*, 47-61.

7. Muth, A.; Madan, M.; Archer, J. J.; Ocampo, N.; Rodriguez, L.; Phanstiel, O., Polyamine transport inhibitors: design, synthesis, and combination therapies with difluoromethylornithine. *J Med Chem* **2014,** *57* (2), 348-363.

8. Pegg, A. E., Mammalian polyamine metabolism and function. *IUBMB Life* **2009,** *61* (9), 880-894.

9. Pegg, A. E., Polyamine metabolism and its importance in neoplastic growth and a target for chemotherapy. *Cancer Res* **1988,** *48* (4), 759-774.

10. Massaro, C.; Thomas, J.; Phanstiel, O., Investigation of Polyamine Metabolism and Homeostasis in Pancreatic Cancers. *Med Sci (Basel)* **2017,** *5* (4), 32.

11. Shirahata, A.; Takahashi, N.; Beppu, T.; Hosoda, H.; Samejima, K., Effects of inhibitors of spermidine synthase and spermine synthase on polyamine synthesis in rat tissues. *Biochem Pharmacol* **1993,** *45* (9), 1897-1903.

12. He, Y.; Shimogori, T.; Kashiwagi, K.; Shirahata, A.; Igarashi, K., Inhibition of cell growth by combination of alpha-difluoromethylornithine and an inhibitor of spermine synthase. *J Biochem* **1995,** *117* (4), 824-829.

13. Lakanen, J. R.; Pegg, A. E.; Coward, J. K., Synthesis and biochemical evaluation of adenosylspermidine, a nucleoside-polyamine adduct inhibitor of spermidine synthase. *J Med Chem* **1995,** *38* (14), 2714-2727.

14. Gitto, S. B.; Pandey, V.; Oyer, J. L.; Copik, A. J.; Hogan, F. C.; Phanstiel, O.; Altomare, D. A., Difluoromethylornithine Combined with a Polyamine Transport Inhibitor Is Effective against Gemcitabine Resistant Pancreatic Cancer. *Mol Pharm* **2018,** *15* (2), 369-376.

15. Kongpracha, P.; Nagamori, S.; Wiriyasermkul, P.; Tanaka, Y.; Kaneda, K.; Okuda, S.; Ohgaki, R.; Kanai, Y., Structure-activity relationship of a novel series of inhibitors for cancer type transporter L-type amino acid transporter 1 (LAT1). *J Pharmacol Sci* **2017,** *133* (2), 96-102.

16. Nefzi, A.; Giulianotti, M. A.; Houghten, R. A., Solid-Phase Synthesis of Substituted 2,3-Diketopiperazines from Reduced Polyamides. *Tetrahedron* **2000,** *56*, 3319-3326.

17. Alhonen-Hongisto, L.; Seppanen, P.; Janne, J., Intracellular putrescine and spermidine deprivation induces increased uptake of the natural polyamines and methylglyoxal bis(guanylhydrazone). *Biochem J* **1980,** *192* (3), 941-945.

18. Burns, M. R.; Carlson, C. L.; Vanderwerf, S. M.; Ziemer, J. R.; Weeks, R. S.; Cai, F.; Webb, H. K.; Graminski, G. F., Amino acid/spermine conjugates: polyamine amides as potent spermidine uptake inhibitors. *J Med Chem* **2001,** *44* (22), 3632-3644.

19. Wang, C.; Delcros, J. G.; Biggerstaff, J.; Phanstiel, O. t., Synthesis and biological evaluation of N1-(anthracen-9-ylmethyl)triamines as molecular recognition elements for the polyamine transporter. *J Med Chem* **2003,** *46* (13), 2663-2671.

20. Gardner, R. A.; Delcros, J. G.; Konate, F.; Breitbeil, F., 3rd; Martin, B.; Sigman, M.; Huang, M.; Phanstiel, O., N1-substituent effects in the selective delivery of polyamine conjugates into cells containing active polyamine transporters. *J Med Chem* **2004,** *47* (24), 6055-6069.

21. Napolitano, L.; Galluccio, M.; Scalise, M.; Parravicini, C.; Palazzolo, L.; Eberini, I.; Indiveri, C., Novel insights into the transport mechanism of the human amino acid transporter LAT1 (SLC7A5). Probing critical residues for substrate translocation. *Biochim Biophys Acta* **2017,** *1861* (4), 727-736.

22. Singh, N.; Ecker, G. F., Insights into the Structure, Function, and Ligand Discovery of the Large Neutral Amino Acid Transporter 1, LAT1. *Int J Mol Sci* **2018,** *19* (5).

23. Muth, A.; Kamel, J.; Kaur, N.; Shicora, A. C.; Ayene, I. S.; Gilmour, S. K.; Phanstiel, O. t., Development of polyamine transport ligands with improved metabolic stability and selectivity against specific human cancers. *J Med Chem* **2013,** *56* (14), 5819-5828.

24. Hafliger, P.; Graff, J.; Rubin, M.; Stooss, A.; Dettmer, M. S.; Altmann, K. H.; Gertsch, J.; Charles, R. P., The LAT1 inhibitor JPH203 reduces growth of thyroid carcinoma in a fully immunocompetent mouse model. *J Exp Clin Cancer Res* **2018,** *37* (1), 234.

25. Obrist, F.; Michels, J.; Durand, S.; Chery, A.; Pol, J.; Levesque, S.; Joseph, A.; Astesana, V.; Pietrocola, F.; Wu, G. S.; Castedo, M.; Kroemer, G., Metabolic vulnerability of cisplatin-resistant cancers. *EMBO J* **2018,** *37* (14), e98597.

26. Wright, P. S.; Byers, T. L.; Cross-Doersen, D. E.; McCann, P. P.; Bitonti, A. J., Irreversible inhibition of S-adenosylmethionine decarboxylase in Plasmodium falciparum-infected erythrocytes: growth inhibition in vitro. *Biochem Pharmacol* **1991,** *41* (11), 1713-1718.

27. Pegg, A. E.; McCann, P. P., S-adenosylmethionine decarboxylase as an enzyme target for therapy. *Pharmacol Ther* **1992,** *56* (3), 359-377.

28. Weeks, R. S.; Vanderwerf, S. M.; Carlson, C. L.; Burns, M. R.; O'Day, C. L.; Cai, F.; Devens, B. H.; Webb, H. K., Novel lysine-spermine conjugate inhibits polyamine transport and inhibits cell growth when given with DFMO. *Exp Cell Res* **2000,** *261* (1), 293-302.

29. Yanagida, O.; Kanai, Y.; Chairoungdua, A.; Kim, D. K.; Segawa, H.; Nii, T.; Cha, S. H.; Matsuo, H.; Fukushima, J.; Fukasawa, Y.; Tani, Y.; Taketani, Y.; Uchino, H.; Kim, J. Y.; Inatomi, J.; Okayasu, I.; Miyamoto, K.; Takeda, E.; Goya, T.; Endou, H., Human L-type amino acid transporter 1 (LAT1): characterization of function and expression in tumor cell lines. *Biochim Biophys Acta* **2001,** *1514* (2), 291-302.

30. Uemura, T.; Yerushalmi, H. F.; Tsaprailis, G.; Stringer, D. E.; Pastorian, K. E.; Hawel, L., 3rd; Byus, C. V.; Gerner, E. W., Identification and characterization of a diamine exporter in colon epithelial cells. *J Biol Chem* **2008,** *283* (39), 26428-26435.

31. Driscoll, D. R.; Karim, S. A.; Sano, M.; Gay, D. M.; Jacob, W.; Yu, J.; Mizukami, Y.; Gopinathan, A.; Jodrell, D. I.; Evans, T. R.; Bardeesy, N.; Hall, M. N.; Quattrochi, B. J.; Klimstra, D. S.; Barry, S. T.; Sansom, O. J.; Lewis, B. C.; Morton, J. P., mTORC2 Signaling

Drives the Development and Progression of Pancreatic Cancer. *Cancer Res* **2016,** *76* (23), 6911-6923.

32. Dai, Z.-J.; Gao, J.; Ma, X.-B.; Kang, H.-F.; Wang, B.-F.; Lu, W.-F.; Lin, S. C.; Wang, X.-J.; Wu, W.-Y., Antitumor Effects of Rapamycin in Pancreatic Cancer Cells by Inducing Apoptosis and Autophagy. *Int. J. Mol. Sci.* **2013,** *14*, 273-285.

33. Napolitano, L.; Scalise, M.; Koyioni, M.; Koutentis, P.; Catto, M.; Eberini, I.; Parravicini, C.; Palazzolo, L.; Pisani, L.; Galluccio, M.; Console, L.; Carotti, A.; Indiveri, C., Potent inhibitors of human LAT1 (SLC7A5) transporter based on dithiazole and dithiazine compounds for development of anticancer drugs. *Biochem Pharmacol* **2017,** *143*, 39-52.

34. Huttunen, K. M.; Gynther, M.; Huttunen, J.; Puris, E.; Spicer, J. A.; Denny, W. A., A Selective and Slowly Reversible Inhibitor of l-Type Amino Acid Transporter 1 (LAT1) Potentiates Antiproliferative Drug Efficacy in Cancer Cells. *J Med Chem* **2016,** *59* (12), 5740-5751.

35. Mosmann, T., Rapid colorimetric assay for cellular growth and survival: application to proliferation and cytotoxicity assays. *J Immunol Methods* **1983,** *65* (1-2), 55-63.

36. Minocha, S. C.; Minocha, R.; Robie, C. A., High-performance liquid chromatographic method for the determination of dansyl-polyamines. *J. Chromatogr.* **1990,** *511*, 177-183.

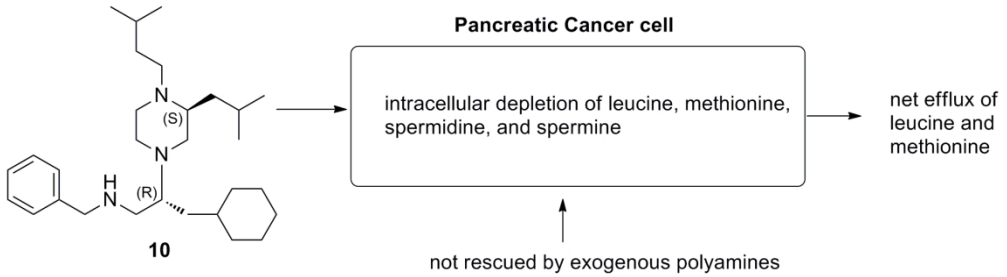

Compound **10** induces efflux of LAT-1 substrates such as leucine and methionine from cells. Methionine depletion results in intracellular depletion of spermidine and spermine, which cannot be rescued by exogenous polyamines.

171x47mm (300 x 300 DPI)